ESD-TR-88-180

Project Report
TT-71

Studies of Target Detection Algorithms That Use Polarimetric Radar Data

L.M. Novak
M.B. Sechtin
M.J. Cardullo

12 October 1988

Lincoln Laboratory

MASSACHUSETTS INSTITUTE OF TECHNOLOGY

LEXINGTON, MASSACHUSETTS

Prepared for the Defense Advanced Research Projects Agency under Electronic Systems Division Contract F19628-85-C-0002.

The work reported in this document was performed at Lincoln Laboratory, a center for research operated by Massachusetts Institute of Technology. This work was sponsored by the Defense Advanced Research Projects Agency under Air Force Contract F19628-85-C-0002 (ARPA Order 3391).

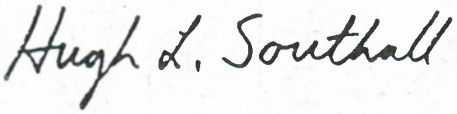

MASSACHUSETTS INSTITUTE OF TECHNOLOGY
LINCOLN LABORATORY

STUDIES OF TARGET DETECTION ALGORITHMS THAT USE POLARIMETRIC RADAR DATA

L.M. NOVAK
M.B. SECHTIN
M.J. CARDULLO
Group 47

PROJECT REPORT TT-71

12 OCTOBER 1988

LEXINGTON MASSACHUSETTS

ABSTRACT

This report describes algorithms which make use of polarimetric radar information in the detection and discrimination of targets in a ground clutter background. The optimal polarimetric detector (OPD) is derived; this algorithm processes the complete polarization scattering matrix (PSM) and provides the best possible detection performance from polarimetric radar data. Also derived is the best linear polarimetric detector, the polarimetric matched filter (PMF), and the structure of this detector is related to simple polarimetric target types. New polarimetric target and clutter models are described; these models are used to predict the performance of the OPD and the PMF. The performance of these algorithms is compared with that of simpler detectors that use only amplitude information to detect targets. Finally, the ability to discriminate between target types by exploiting differences in polarimetric scattering properties is discussed.

TABLE OF CONTENTS

LIST OF ILLUSTRATIONS

LIST OF TABLES

1. EXECUTIVE SUMMARY

Under DARPA sponsorship, M.I.T. Lincoln Laboratory is conducting a broad-based research effort to (1) develop an understanding of the phenomenology of polarimetric radar data and (2) relate this phenomenology to the performance results achievable by target detection and classification algorithms that use polarimetric data. In order to develop the mathematical framework from which optimal polarimetric detectors and classifiers can be derived, a clear understanding of the underlying polarimetric phenomenology is necessary. This understanding is also necessary for predicting and analyzing the performance of various polarimetric detectors and classifiers. This, in turn, will allow the development of viable stationary target detection and classification systems. Such systems have application in surveillance, fire control, and missile-seeker systems. This report summarizes some of the recent work in the area of stationary target detection and classification using polarimetric radar information.

To investigate the detection and classification performance improvement achievable through the use of fully polarimetric radar data, statistical models of targets and clutter were first developed based on available polarimetric target and clutter data. From these models, new algorithms were derived for optimal processing of the polarimetric radar data. These new algorithms, the optimal polarimetric detector (OPD) and polarimetric-matched filter (PMF), were compared with a variety of non-polarimetric algorithms which use only single-polarimetric-channel returns to detect targets. Detection performance predictions for radars using circularly polarized data were also presented.

Based upon a limited polarimetric clutter data base and a target data base of turntable measurements, our performance predictions show that the target detection performance achievable using the OPD or the PMF is not significantly better than that which is achievable using simpler, single-polarimetric-channel radar detectors. Furthermore, to implement the OPD or PMF requires prior knowledge of target and clutter statistics; this would be difficult, since clutter statistics vary widely and are highly unpredictable.

Although polarization information may not improve detection performance, it may be useful in target classification. Some target types have distinctive polarimetric scattering properties. Preliminary studies using an optimal polarimetric classifier suggest that the polarimetric properties could be exploited to discriminate among target types (e.g., armored targets vs. trucks).

It is again emphasized that the clutter data base which the results of this report are based on is very limited; a more comprehensive set of measurements of various clutter types (e.g., snow-covered terrain) must be obtained and analyzed. In the very near future we plan to collect this

comprehensive clutter data base using the Advanced Detection Technology Sensor (ADTS), and to verify the tentative conclusions of this report using the new data base. The mathematical framework necessary to perform these future studies is provided in this report, along with the new polarimetric detection and classification algorithms for optimally processing the fully polarimetric radar data.

1.1 INTRODUCTION

The detection of stationary targets in ground clutter is an important problem for both strategic and tactical applications. In an earlier program, the Hostile Weapons Location System (HOWLS) Program [1, 2], M.I.T. Lincoln Laboratory investigated the detection performance that could be achieved using a single-polarimetric-channel radar with a resolution on the order of the size of a typical target (10 m by 10 m). The radar employed pulse-to-pulse frequency diversity; this was used to obtain independent samples of targets and clutter which could then be noncoherently integrated. Statistical target and clutter models based on analysis of the collected radar data were developed. These models were used to develop performance predictions for various non-polarimetric detection algorithms. These predictions were found to agree reasonably well with the performance achieved by the actual algorithms.

Could HOWLS detection performance have been improved if the radar had been fully polarimetric, and if the full polarization scattering matrix (PSM) had been used in the detection algorithms? This report addresses that question.

To measure the full PSM, a radar must transmit two orthogonal polarizations at each frequency. Therefore, in this report we assume horizontal polarization is transmitted first and two linear orthogonal polarizations (denoted HH and HV) are received. Next, vertical polarization is transmitted and two linear orthogonal polarizations (denoted VV and VH) are received. By reciprocity VH = HV, and therefore the three complex elements HH, HV, and VV comprise the total information contained in the polarization scattering matrix. For multi-look algorithms, successive independent PSM measurements are obtained using frequency diversity.

In order to investigate the possible contribution to detection from the fully polarimetric data, we extended the target and clutter statistical models to the fully polarimetric case. Then we developed detection algorithms which use this information. Finally, we developed formulas for predicting the performance of these algorithms, and used these formulas to evaluate and compare the various detection algorithms.

In Section 2 we introduce the basic polarimetric measurement model and develop homogeneous statistical models of targets and clutter. These statistical models are used to evaluate the predicted performance of various polarimetric and non-polarimetric detection algorithms.

In Section 3 we use these homogeneous target and clutter models to derive the optimal polarimetric detector (OPD). This algorithm reveals the structure of the detector which yields the best performance under ideal conditions; that is, it provides an upper bound on detection performance for the homogeneous case.

Section 4 develops the concept of a polarimetric matched filter (PMF). This is the linear processor that processes the complex polarimetric returns (HH, HV and VV) so as to provide maximum target-to-clutter ratio to the detector. A useful interpretation of the solution of the PMF is shown to correspond to simple dihedral and trihedral reflector types.

In Section 5 we present several alternative detection algorithms. These algorithms are suboptimal because they ignore some of the polarimetric information; they are, however, independent of the parameters of the target and clutter whereas the OPD and the PMF require exact knowledge of the target and clutter statistics. The algorithms considered include the polarimetric span and various single-polarimetric-channel detectors.

Section 6 develops more realistic target and clutter models. In this section it is assumed that clutter is spatially nonhomogeneous and that target returns vary with aspect angle. Random polarimetric target and clutter models having a product-model structure are postulated; such models are consistent with these more realistic assumptions. The exact probability density function (PDF) for product-model targets and clutter is derived; these PDFs are used to obtain the optimal likelihood-ratio detector for product-model targets and clutter.

Section 7 develops the mathematical formulas used for predicting the performance of various detection algorithms introduced in Sections 3, 4, and 5. The analysis uses the product-model characterizations of targets and clutter developed in Section 6. The detection algorithms analyzed include the OPD, the PMF, and single-polarimetric-channel detectors. In these analyses the performance predictions for homogeneous targets and clutter are obtained as a special case of the more general product-model solution.

Section 8 introduces the concept of a radar which uses a single-transmit, dual-receive configuration with a circular polarization basis. This scheme is predicated on the empirical observation that armored targets tend to have a significant amount of even-bounce (LL) return whereas clutter tends to have mostly odd-bounce (LR) return. Thus, circular polarization is used to take advantage of this difference. Section 8 parallels the previous sections 3 through 7. That is, for this circular polarization case, an OPD and PMF are derived, as well as alternative suboptimal detectors. Then the product-model characterizations of targets and clutter are used to derive formulas for performance predictions of the various algorithms.

Finally, in Section 9 a comparison of the detection performance of various polarimetric and non-polarimetric detectors is presented. The comparisons presented include (1) a comparison of the OPD, span and single-channel $|HH|^2$ detectors, (2) a comparison of the PMF and single-channel $|HH|^2$ and $|LL|^2$ detectors, and (3) a comparison of the OPD and dual-circular detection algorithms. Also, we examine the performance of the OPD when it is used as a target classifier.

Section 10 summarizes the findings of these studies and describes some possible future study efforts.

2. THE BASIC POLARIMETRIC MEASUREMENT MODEL

This section describes the basic mathematical modeling of targets and clutter used in our studies. These models are used in the later sections to derive the optimal polarimetric detector and the polarimetric matched filter.

We express the radar return as the polarimetric feature vector $\underline{X}$, where

$$\underline{X} = \begin{bmatrix} HH_i + jHH_q \\ HV_i + jHV_q \\ VV_i + jVV_q \end{bmatrix} = \begin{bmatrix} HH \\ HV \\ VV \end{bmatrix} \tag{1}$$

Each complex element HH, HV, and VV is modeled as having a complex-Gaussian probability density function (PDF). The joint PDF of vector $\underline{X}$ is given by the expression

$$f(\underline{X}) = \frac{1}{\pi^n |\Sigma|} \exp\left\{-\underline{X}^\dagger \Sigma^{-1} \underline{X}\right\} \tag{2}$$

where $\Sigma = E\{\underline{X}\ \underline{X}^\dagger\}$ is the covariance of the polarimetric feature vector. The data have a zero-mean ($E\{\underline{X}\} = \underline{0}$). Thus, the complete characterization of the jointly Gaussian complex elements HH, HV, and VV is given in terms of an appropriate covariance matrix Σ. The covariance matrices which we use for target and clutter data (in a linear polarization basis) are [3, 4] of the form

$$\Sigma = \sigma \left[\begin{array}{c|c|c} 1 & 0 & \rho\sqrt{\gamma} \\ \hline 0 & \epsilon & 0 \\ \hline \rho^*\sqrt{\gamma} & 0 & \gamma \end{array}\right] \tag{3}$$

$$\text{where} \quad \sigma = E\{|HH|^2\}, \quad \epsilon = \frac{E\{|HV|^2\}}{E\{|HH|^2\}}, \quad \gamma = \frac{E\{|VV|^2\}}{E\{|HH|^2\}} \tag{4}$$

$$\text{and} \quad \rho\sqrt{\gamma} = \frac{E\{HH\ VV^*\}}{E\{|HH|^2\}}$$

The clutter covariance is specified by four parameters (σ_c, ϵ_c, γ_c, ρ_c) and the target covariance is also specified by four parameters (σ_t, ϵ_t, γ_t, ρ_t). Also, since the target is in a clutter background, the measured target data are modeled (by superposition) as

$$\underline{X}_{t+c} = \underline{X}_t + \underline{X}_c \tag{5}$$

This implies that the target-plus-clutter data are also zero-mean and complex-Gaussian with covariance

$$\Sigma_{t+c} = \Sigma_t + \Sigma_c \tag{6}$$

and thus has the same structure as given in Equation (3) above, with

$$\begin{aligned}
\sigma_{t+c} &= \sigma_t + \sigma_c \\
\epsilon_{t+c} &= \frac{\sigma_t\epsilon_t + \sigma_c\epsilon_c}{\sigma_{t+c}} \\
\gamma_{t+c} &= \frac{\sigma_t\gamma_t + \sigma_c\gamma_c}{\sigma_{t+c}} \\
\rho_{t+c}\sqrt{\gamma_{t+c}} &= \frac{\sigma_t\rho_t\sqrt{\gamma_t} + \sigma_c\rho_c\sqrt{\gamma_c}}{\sigma_{t+c}}
\end{aligned} \tag{7}$$

Finally, the input target-to-clutter ratio is defined

$$(T/C)_{in} = \frac{\sigma_t}{\sigma_c} \tag{8}$$

3. THE OPTIMAL POLARIMETRIC DETECTOR

In this section we will derive the optimal polarimetric detector (OPD) for the ideal situation, that is, assuming the parameters (σ, ϵ, γ, ρ) and the target-to-clutter ratio $(T/C)_{in}$ are known exactly. The algorithm we obtain will reveal the structure of the detector that provides the best possible detection performance achievable under ideal conditions. The performance of this ideal optimal detector will provide an upper bound against which other polarimetric and non-polarimetric detection schemes can be compared. For our two-class problem (i.e., target-plus-clutter versus clutter) the likelihood ratio test for the presence of a target is [5]

$$\frac{f(\underline{X} \mid \omega_{t+c})}{f(\underline{X} \mid \omega_c)} > T_D \tag{9}$$

where we denote the target-plus-clutter class by ω_{t+c} and the clutter only class by ω_c. T_D is the detection threshold. The likelihood ratio has been shown [4] to be a quadratic detector of the form

$$\underline{X}^\dagger \left(\Sigma_c^{-1} - \Sigma_{t+c}^{-1}\right)\underline{X} + \ln \frac{|\Sigma_c|}{|\Sigma_{t+c}|} > \ln T_D \tag{10}$$

Substituting particular covariance matrices defining two classes (target-plus-clutter and clutter in our examples) into the above algorithm yields an interesting result. Rewriting the above solution in a slightly different form, the optimal detector uses the distances to the target-plus-clutter class and the clutter class in the following test:

$$d_c(\underline{X}) - d_{t+c}(\underline{X}) > \ln T_D \tag{11}$$

where

$$d_c(\underline{X}) = \underline{X}^\dagger \Sigma_c^{-1} \underline{X} + \ln |\Sigma_c| \tag{12}$$

and

$$d_{t+c}(\underline{X}) = \underline{X}^\dagger \Sigma_{t+c}^{-1} \underline{X} + \ln |\Sigma_{t+c}| \tag{13}$$

Evaluating the above distance measures, one obtains an expression for the detection statistic [6]

$$d_i(\underline{X}) = \frac{|HH|^2}{\sigma_i(1 - |\rho_i|^2)} + \frac{|VV|^2}{\sigma_i(1 - |\rho_i|^2)\gamma_i} + \frac{|HV|^2}{\sigma_i \epsilon_i} \qquad (14)$$

$$- \frac{2|\rho_i|}{\sigma_i(1 - |\rho_i|^2)\sqrt{\gamma_i}} |HH| \, |VV| \cos(\phi_{HH} - \phi_{VV} - \phi_{\rho_i})$$

$$+ \ln \sigma_i \epsilon_i \gamma_i^3 (1 - |\rho_i|^2) \quad ; \; i = c, \; t + c$$

where ϕ_{HH}, ϕ_{VV}, and ϕ_{ρ_i} are the phase terms of the complex quantities HH, VV, and ρ_i, respectively. The fundamental structure of the optimal polarimetric detector makes use of the polarimetric amplitude information ($|HH|$, $|HV|$, $|VV|$); the detector also makes use of the polarimetric phase difference ($\phi_{HH} - \phi_{VV}$), which corresponds to the difference in phase between the HH and VV complex returns. The OPD applies optimal weighting [as shown in Equation (14) above] to the observed radar measurement data prior to making its detection decision.

4. THE POLARIMETRIC MATCHED FILTER

In the previous section of the report we defined the two-class target detection problem and derived the detection algorithm which makes optimal use of the observed polarimetric return. This algorithm is optimal in the likelihood-ratio sense; that is, it yields the best possible probability of detection (P_D) for a given false alarm probability (P_{FA}). An alternative approach is to design a linear processor or matched filter, which processes the polarimetric return so as to provide maximum target-to-clutter ratio to the radar detector. We will call this algorithm a polarimetric matched filter (PMF); it is easily derived using the approach given in Reference 7. A brief derivation of this detector is given below.

Again the assumption is that we have two classes (the target-plus-clutter class and the clutter class) but we now seek the best set of linear weighting coefficients for processing the polarimetric data vector. That is, we seek the linear combination $y = \underline{h}^{\dagger}\underline{x}$ which provides the maximum target-to-clutter ratio at the filter output. This ratio is given by

$$(T/C)_{out} = \frac{\underline{h}^{\dagger}\Sigma_t\underline{h}}{\underline{h}^{\dagger}\Sigma_c\underline{h}} \tag{15}$$

The polarimetric matched filter makes use of the target and clutter covariances Σ_t and Σ_c. This implies a design which is independent of the actual input target-to-clutter ratio; i.e., the PMF is a constant-coefficient filter.

It is well known [7] that the optimal weight vector, denoted $\underline{h}^*$, is obtained as the solution to the generalized eigenvalue problem

$$\Sigma_t\underline{h}^* = \lambda^*\Sigma_c\underline{h}^* \tag{16}$$

where $\underline{h}^*$ is the eigenvector corresponding to the maximum eigenvalue, λ^*. Also, the maximum eigenvalue λ^* is actually the optimal target-to-clutter ratio out of the filter which is obtained as a result of using the optimal $\underline{h}^*$. Equivalently, one may obtain the $(\lambda^*, \underline{h}^*)$ solution by solving the following simpler eigenvalue-eigenvector problem:

$$\Sigma_c^{-1}\Sigma_t\ \underline{h}^* = \lambda^*\underline{h}^* \tag{17}$$

It is more convenient to solve this equivalent eigenvalue problem since the structure of the matrix $\Sigma_c\ \Sigma_t$ is simple and easily leads to an exact analytical solution.

Specifically, we find

$$\Sigma_c^{-1}\Sigma_t = \frac{\sigma_t}{\sigma_c(1-\rho_c^2)\epsilon_c\gamma_c}\begin{bmatrix} \epsilon_c(\gamma_c - \sqrt{\gamma_c}\sqrt{\gamma_t}\rho_c\rho_t) & 0 & \epsilon_c(\gamma_c\sqrt{\gamma_t}\rho_t - \gamma_t\sqrt{\gamma_c}\rho_c) \\ 0 & \epsilon_t(1-\rho_c^2)\gamma_c & 0 \\ \epsilon_c(\rho_t\sqrt{\gamma_t} - \rho_c\sqrt{\gamma_c}) & 0 & \epsilon_c(\gamma_t - \sqrt{\gamma_c}\sqrt{\gamma_t}\rho_c\rho_t) \end{bmatrix} \quad (18)$$

Although the above matrix is not symmetric, it has been shown [7] that the eigenvalues are all positive. In evaluating the eigenvalues and eigenvectors of Equation (18), we first simplify the solution by omitting the scale factor $\sigma_t/\sigma_c(1-\rho_c^2)\epsilon_c\gamma_c$ since the eigenvectors are independent of this scale factor. We then determine the (normalized) eigenvalues and their corresponding eigenvectors. The results of this analysis are summarized as follows:

1. The (normalized) eigenvalue $\lambda_1 = \epsilon_t\gamma_c(1-\rho_c^2)$ has the eigenvector

$$h_1 = \begin{bmatrix} 0 \\ 1 \\ 0 \end{bmatrix} \quad (19)$$

2. The remaining (normalized) eigenvalues λ_2, λ_3 are found to be

$$\lambda_2 = 0.5\,\epsilon_c\Big[-\sqrt{\gamma_c\gamma_t\,4\rho_t^2 + 4\rho_c^2 - 2 - 4\sqrt{\gamma_c}\gamma_t^{3/2}\rho_c\rho_t - 4\sqrt{\gamma_t}\gamma_c^{3/2}\rho_c\rho_t + \gamma_t^2 + \gamma_c^2} - 2\sqrt{\gamma_c}\sqrt{\gamma_t}\rho_c\rho_t + \gamma_t + \gamma_c\Big] \quad (20)$$

$$\lambda_3 = 0.5\,\epsilon_c\Big[+\sqrt{\gamma_c\gamma_t\,4\rho_t^2 + 4\rho_c^2 - 2 - 4\sqrt{\gamma_c}\gamma_t^{3/2}\rho_c\rho_t - 4\sqrt{\gamma_t}\gamma_c^{3/2}\rho_c\rho_t + \gamma_t^2 + \gamma_c^2}$$

$$-2\sqrt{\gamma_c}\sqrt{\gamma_t}\rho_c\rho_t + \gamma_t + \gamma_c\Big] \qquad (21)$$

Thus the three eigenvectors obtained for the above matrix are of the form

$$\underline{h}_1 = \begin{bmatrix}0\\1\\0\end{bmatrix}, \quad \underline{h}_2 = \begin{bmatrix}1\\0\\\beta_2\end{bmatrix}, \quad \underline{h}_3 = \begin{bmatrix}1\\0\\\beta_3\end{bmatrix} \qquad (22)$$

where the parameters β_2 and β_3 are given by the expression

$$\beta_{2,3} = \pm\sqrt{\frac{\left[4\gamma_c\gamma_t\rho_t^2 - 4\sqrt{\gamma_c}\gamma_t^{3/2}\rho_c\rho_t - 4\sqrt{\gamma_t}\gamma_c^{3/2}\rho_c\rho_t + 4\gamma_c\gamma_t\rho_c^2+\gamma_t^2 - 2\gamma_c\gamma_t+\gamma_c^2\right]+\gamma_t-\gamma_c}{2\gamma_c\sqrt{\gamma_t}\rho_t - 2\sqrt{\gamma_c}\gamma_t\rho_c}} \qquad (23)$$

The optimal polarimetric matched filter corresponds to one of the three solutions in Equation (22); in particular, it corresponds to the solution defined by the maximum of the three eigenvalues λ_1, λ_2, λ_3. Thus the polarimetric matched filter is one of the three possible linear combinations of the polarimetric measurements, namely

$$\begin{aligned}
&\text{(i)} \quad y_1 = HV \\
&\text{(ii)} \quad y_2 = HH + \beta_2 VV \qquad (24)\\
&\text{(iii)} \quad y_3 = HH + \beta_3 VV
\end{aligned}$$

To gain further insight into the above solution, we will consider the behavior of the solution for the cases $\beta = \pm 1$. These solutions are related to simple types of radar reflectors. For the special case when $\gamma_t = \gamma_c = 1$, the optimal polarization combinations become

$$\begin{aligned}
&\text{(i)} \quad y_1 = HV \\
&\text{(ii)} \quad y_2 = HH + VV \qquad (25)\\
&\text{(iii)} \quad y_3 = HH - VV
\end{aligned}$$

These three solutions correspond to the following simple target-in-clutter situations

(i) HV is the polarization measurement that has the maximum signal return for a dihedral reflector oriented at ±45° relative to the horizontal.

(ii) HH + VV is the polarization measurement combination that has the maximum signal return for a trihedral reflector.

(iii) HH - VV is the polarization measurement combination that has the maximum signal return for a dihedral reflector oriented horizontally or vertically.

5. ALTERNATIVE DETECTION ALGORITHMS

Sections 3 and 4 discussed two approaches (the optimal polarimetric detector and the polarimetric matched filter) to detecting targets in clutter. Both of these approaches are dependent on the parameters of the target and clutter classes. There are other approaches to detecting targets in clutter that are independent of the parameters of the target and clutter classes. These detection algorithms are suboptimal because they ignore some of the polarimetric information. We will consider several of these methods.

The first scheme (used extensively in various radar applications by numerous researchers) processes the complex radar return by computing the polarimetric span according to the relation

$$y = |HH|^2 + 2|HV|^2 + |VV|^2 \tag{26}$$

The span detection statistic makes use of the total power in the polarimetric return and has the property of being invariant with respect to the polarization basis used by the radar. The span is actually a suboptimal quadratic detector, since it is obtained from the simplified algorithm

$$y = (HH^*, HV^*, VV^*) \begin{bmatrix} 1 & 0 & 0 \\ 0 & 2 & 0 \\ 0 & 0 & 1 \end{bmatrix} \begin{bmatrix} HH \\ HV \\ VV \end{bmatrix} > T_D \tag{27}$$

Note that the span detector does not make use of the polarimetric phase $(\phi_{HH} - \phi_{VV})$. Since the span detector utilizes only the polarimetric amplitude information, using it will provide some insight from the comparison of performance results for the various algorithms as to the usefulness of polarimetric phase in our target detection application. We will also consider single polarimetric channel radars (specifically, HH, LL, and LR) and will compare the performance of these simpler algorithms to that of the more complex algorithms. Finally, we will evaluate the performance of a single circular transmit, dual circular receive radar system. This scheme makes use of both LL and LR polarimetric returns and we will compare the performance of this system to the performance achieved using the full PSM system.

6. PRODUCT TARGET AND CLUTTER MODELS

The previous sections presented a number of polarimetric and non-polarimetric detectors, namely,

1. The optimal polarimetric detector (OPD)
2. The polarimetric matched filter (PMF)
3. The span detector
4. Single-channel (non-polarimetric) detectors

This section develops more realistic target and clutter models; these will be used in the next section to evaluate the detection performance of these algorithms and their sensitivity to non-Gaussian distributions of targets and clutter.

Until now we have assumed a homogeneous clutter background; as a result each clutter pixel in the scene had the same average polarimetric power and the same covariance between the polarimetric returns. Also, we assumed the target-plus-clutter samples to be from a single Gaussian PDF (probability density function) with a constant average power and covariance. It is more realistic to assume that (a) the clutter background is spatially nonhomogeneous, and (b) the target returns vary with aspect angle. To this end, in this section we postulate random polarimetric target and clutter models consistent with these more realistic assumptions. Specifically, we postulate random polarimetric target and clutter models having a product-model structure. This enables us to evaluate the effects of spatial variability of clutter and aspect angle variability of targets on the performance of the optimal polarimetric detector, the polarimetric matched filter, and the other, simpler detectors. To compare these detectors, we also need an optimal likelihood-ratio detector for the product models of targets and clutter. Therefore, we also derive the exact PDF for the product model polarimetric feature vectors and implement the likelihood ratio detector for the product model problem.

Since we are interested in a product model for both targets and clutter, we take the model to be of the form

$$\underline{y} = \sqrt{\alpha}\underline{X} \tag{28}$$

where $\sqrt{\alpha}$ represents an arbitrary scale factor. Our basic assumptions are (1) that the feature vectors $\underline{X}$ have a specified covariance matrix Σ and (2) that the vectors $\underline{X}$ are scaled according to some random variable $\sqrt{\alpha}$. This defines our product model for polarimetric data measurements and represents a simple extension of the single-polarimetric-channel product models of targets and clutter derived in Reference 1. Determining the PDF of random vector $\underline{y}$ is straightforward and proceeds as described below.

For a given value α, we have

$$E\{\underline{y}/\alpha\} = \sqrt{\alpha}E\{\underline{X}\} = \underline{0} \tag{29}$$

$$COV\ \{\underline{y}/\alpha\} = \alpha\sum \tag{30}$$

Since the vector $\underline{X}$ is assumed to be complex-Gaussian, the conditional PDF of random vector $\underline{y}$ is also complex-Gaussian

$$f(\underline{y}/\alpha) = \frac{1}{\pi^n \alpha^n |\sum|} \exp\left\{-\frac{\underline{y}^\dagger \sum^{-1} \underline{y}}{\alpha}\right\} \tag{31}$$

Next, we compute the unconditional PDF of random vector $\underline{y}$ which is obtained from the integral

$$f(\underline{y}) = \int_0^\infty f(\underline{y}/\alpha)\ p(\alpha)\ d\alpha \tag{32}$$

where $p(\alpha)$ is the PDF of the scalar product multiplier. In References 8, 9, and 10, a Gamma (or chi-square) distributed cross-section model was assumed having density

$$p(\alpha) = \frac{1}{\bar{\alpha}}\left(\frac{\alpha}{\bar{\alpha}}\right)^{\nu-1} \frac{1}{\Gamma(\nu)} \exp\left\{-\frac{\alpha}{\bar{\alpha}}\right\} \tag{33}$$

In this two-parameter cross-section model, ν is the order parameter and $\bar{\alpha}$ is related to the mean radar cross-section. This has been shown [8, 9, 10] to yield the K-distribution for single polarimetric-channel ground clutter and sea clutter. We have shown that this distribution is a reasonable model for both radar ground clutter and targets similar to that data collected using the HOWLS [1] radar. We will apply this cross-section model to the polarimetric feature vector problem and will show that this leads to a generalized K-distribution for the PDF of random vector $\underline{y}$. Substituting Equations (31) and (33) into Equation (32), we obtain the result

$$f(\underline{y}) = \frac{1}{\pi^n \bar{\alpha}^\nu \Gamma(\nu) |\sum|} \int_0^\infty \alpha^{n-\nu-1} \exp\left\{-\alpha \underline{y}^\dagger \sum^{-1} \underline{y}\right\} \exp\left\{-\frac{1}{\alpha\bar{\alpha}}\right\} d\alpha \tag{34}$$

Using tabulated integrals from Reference 11, we obtain the result

$$f(\underline{y}) = \frac{2}{\pi^n \bar{\alpha}^\nu \Gamma(\nu) |\sum|} \frac{K_{n-\nu}\left(2\sqrt{\dfrac{\underline{y}^\dagger \sum^{-1} \underline{y}}{\bar{\alpha}}}\right)}{(\bar{\alpha}\underline{y}^\dagger \sum^{-1} \underline{y})^{(n-\nu)/2}} \tag{35}$$

Given this exact PDF for the product model characterization of targets and clutter, we next obtain the corresponding optimal log-likelihood ratio detector. Omitting the details, we obtain the distance measures $D_{t+c}(\underline{y})$ and $D_c(\underline{y})$

$$D_i(\underline{y}) = (\nu_i - n) \ln (d_i^2/2\bar{\alpha}_i) + \ln K_{\nu_i - n}\left(2\sqrt{\frac{d_i^2}{2\bar{\alpha}_i}}\right)$$

$$- \ln\Gamma(\nu_i) - \ln |\Sigma_i| - \nu_i \ln \bar{\alpha}_i \qquad (36)$$

$$\text{where } d_i^2 = \underline{y}^\dagger \Sigma_i^{-1} \underline{y} \quad ; \quad i = c,\ t + c$$

The optimal polarimetric detector for product-model targets and clutter determined by Equation (36) has the same form as Equation (11); i.e., the optimal test for the presence of a target is

$$D_c(\underline{y}) - D_{t+c}(\underline{y}) > \ln T_D \qquad (37)$$

We will use this detector in the ideal situation--where the parameters (σ, ϵ, γ, ρ) and the target-to-clutter ratio are known exactly and the parameters (ν, $\bar{\alpha}$) are also known exactly. The performance of this detector therefore will provide an upper bound against which we can compare the performance of our other detectors. In this way, we may judge the relative degradation in performance which occurs when the detectors are designed for some nominal target and clutter parameters but tested against product model input data.

7. SENSITIVITY ANALYSIS OF POLARIMETRIC ALGORITHMS

In the previous sections, we derived polarimetric and non-polarimetric detectors for homogeneous (Gaussian) target and clutter statistics. In this section, the actual test inputs will be assumed to have a product model structure, and the sensitivity of the detectors to the effects of clutter spatial variability and target aspect-angle variability will be determined.

7.1 ANALYSIS OF THE OPD - SINGLE-LOOK SOLUTION

For the optimal polarimetric detector, we write

$$y = \underline{X}^{\dagger}(\Sigma_c^{-1} - \Sigma_{t+c}^{-1})\,\underline{X} + C \tag{38}$$

where

$$C = \ln \frac{|\Sigma_c|}{|\Sigma_{t+c}|} - \ln T_D \tag{39}$$

Taking the approach of References 12 and 13, we evaluate the conditional characteristic function of random variable y:

$$\phi_{y/\alpha}(jw) = \int_{-\infty}^{\infty} \cdots \int_{-\infty}^{\infty} \exp\{jw(\underline{X}^{\dagger}[\Sigma_c^{-1} - \Sigma_{t+c}^{-1}]\,\underline{X} + C)\} \frac{\exp\left\{\dfrac{-\underline{X}^{\dagger}\Sigma^{-1}\underline{X}}{\alpha}\right\}}{\pi^n \alpha^n |\Sigma|}\, d\underline{X} \tag{40}$$

The above expression implies that we have designed the detector using nominal Σ_{t+c} and Σ_c for our target-plus-clutter and clutter classes, but are testing the algorithm with measurement data that have a product model structure by appropriately selecting Σ and α. For now, however, we assume a given α and evaluate the exact characteristic function to be of the form

$$\phi_{y/\alpha}(jw) = e^{jwC} \prod_{i=1}^{3} \frac{1}{(1 - j2\alpha\lambda_i w)} \tag{41}$$

where the eigenvalues λ_1, λ_2, λ_3 are obtained from the simultaneous diagonalization of the matrices

$$\Sigma_c^{-1} - \Sigma_{t+c}^{-1} \quad \text{and} \quad \Sigma^{-1} \tag{42}$$

A FORTRAN program which computes the eigenvalues λ_1, λ_2, and λ_3 is included in the Appendix. The eigenvalues are given as analytical closed-form expressions; these expressions were obtained using MACSYMA [14].

Expanding Equation (41) by partial fractions yields

$$\phi_{y/\alpha}(jw) = e^{jwC} \sum_{i=1}^{3} \frac{A_i}{(1-j2\alpha\lambda_i w)} \tag{43}$$

where the residues A_i are simple functions of λ_1, λ_2, and λ_3. Taking the inverse transform yields the conditional probability density

$$f_{y/\alpha}(y) = \sum_{i=1}^{3} A_i f_i(y) \tag{44}$$

where

$$f_i(y) = F^{-1}\left\{\frac{e^{-jwC}}{(1-j2\alpha\lambda_i w)}\right\} \tag{45}$$

Detection and false alarm probabilities are obtained by integrating:

$$P_{D/FA}(\alpha) = \int_0^\infty f(y/\alpha)d\alpha \tag{46}$$

The result is the sum of three integrals

$$P_{D/FA}(\alpha) = \sum_{i=1}^{3} A_i \, P_i(\alpha) \tag{47}$$

where

$$\begin{aligned}
P_i(\alpha) &= 1 - \exp\left\{\frac{C}{2\alpha\lambda_i}\right\} \quad ; \quad \lambda_i > 0,\ C < 0 \\
P_i(\alpha) &= 0 \qquad\qquad\qquad\quad ; \quad \lambda_i > 0,\ C > 0 \\
P_i(\alpha) &= \exp\left\{\frac{C}{2\alpha\lambda_i}\right\} \quad ; \quad \lambda_i < 0,\ C > 0 \\
P_i(\alpha) &= 1 \qquad\qquad\qquad\quad ; \quad \lambda_i < 0,\ C < 0
\end{aligned} \tag{48}$$

The above expressions (47) and (48) are valid for any particular value of α. When α is modeled as a random variable (as it is for the product model), the detection probability is likewise a random variable. An average probability is obtained by averaging with respect to α:

$$\bar{P}_{D/FA} = E_{\alpha}\{P_{D/FA}(\alpha)\} = \sum_{i=1}^{3} A_i E\{P_i(\alpha)\} \tag{49}$$

where

$$E_{\alpha}\{P_i(\alpha)\} = 1 - \left[\frac{-C\bar{\alpha}}{2\lambda_i}\right]^{\nu/2} \frac{K_{\nu}\left(2\sqrt{\frac{-C}{2\lambda_i\bar{\alpha}}}\right)}{\bar{\alpha}^{\nu}\,\Gamma(\nu)} \quad ; \quad \lambda_i > 0,\ C < 0$$

$$E_{\alpha}\{P_i(\alpha)\} = 0 \quad ; \quad \lambda_i > 0,\ C > 0$$

$$E_{\alpha}\{P_i(\alpha)\} = \left[\frac{-C\bar{\alpha}}{2\lambda_i}\right]^{\nu/2} \frac{K_{\nu}\left(2\sqrt{\frac{-C}{2\lambda_i\bar{\alpha}}}\right)}{\bar{\alpha}^{\nu}\,\Gamma(\nu)} \quad ; \quad \lambda_i < 0,\ C > 0 \tag{50}$$

$$E_{\alpha}\{P_i(\alpha)\} = 1 \quad ; \quad \lambda_i < 0,\ C < 0$$

The exact $P_{D/FA}$ performance of the OPD for homogeneous target and clutter models is obtained from Equations (47) and (48) by setting the random multiplier $\alpha = 1$. The exact solution for the detection performance of the OPD involves calculation of the three eigenvalues λ_1, λ_2, λ_3 from simultaneous diagonalization of the covariance matrices of Equation (42) above; this is true for both homogeneous and non-homogeneous inputs. The exact solution to this simultaneous diagonalization problem is given in the Appendix.

7.2 ANALYSIS OF THE OPD - MULTI-LOOK SOLUTION

We are interested in evaluating the performance of the OPD when two or more independent measurements of the polarimetric data, $\underline{X}$, are processed in an optimal manner. In this subsection, the extension of the analysis to the multi-look case is presented. The assumptions we make are (i) that each observed polarimetric measurement vector from class ω_c has the same mean and covariance statistics ($\underline{0}$, Σ_c) and (ii) that each polarimetric measurement vector from class ω_{t+c} has the same statistics ($\underline{0}$, Σ_{t+c}). With these assumptions, it is easy to show that the likelihood ratio test for

m independent observations is equivalent to sequentially processing each observed vector $\underline{X}_i$, i=1,2,...m in the single-look quadratic classifier [15]. The single-look detection statistics y_i are then summed and compared with the detection threshold T_D. Finally, since the characteristic function of a sum of independent random variables is the product of the individual characteristic functions, we obtain for the m-look case

$$\phi^{(m)}_{y/\alpha}(jw) = e^{jwC} \prod_{i=1}^{3} \frac{1}{(1-j2\alpha\lambda_i w)}^{m} \tag{51}$$

From this, one may obtain the exact formulas for detection and false alarm probabilities. The solution is lengthy and only the final results will be given here. Using the partial fraction expansion technique of Reference 16, we obtain the solution

$$P^{(m)}_{D/FA}(\alpha) = \sum_{i=1}^{3} \sum_{\ell=1}^{m} A^{(m)}_{i\ell}\, P^{(m)}_{i\ell} \tag{52}$$

where

$$\begin{aligned} P^{(m)}_{i\ell} &= G_{i\ell}(\alpha) \quad ; \quad \lambda_i > 0,\ c < 0 \\ P^{(m)}_{i\ell} &= 1 \quad ; \quad \lambda_i > 0,\ c > 0 \\ P^{(m)}_{i\ell} &= 1-G_{i\ell}(\alpha) \quad ; \quad \lambda_i < 0,\ c > 0 \\ P^{(m)}_{i\ell} &= 0 \quad ; \quad \lambda_i < 0,\ c < 0 \end{aligned} \tag{53}$$

where

$$G_{i\ell}(\alpha) = \int_{-C/\alpha\lambda_i}^{\infty} \frac{X^{\ell-1} e^{-X/2}}{2^{\ell}(\ell-1)!}\, dx \tag{54}$$

and

$$A_{i\ell} = \frac{(-2\lambda_i)^{\ell}}{(m-\ell)! \prod_{k=1}^{3} (-2\lambda_k)^{m}} \sum_{n=0}^{m-\ell} \binom{m-\ell}{n}$$

$$\frac{[(-m-n+1)(-m-n+2)....(-m)][(-2m+\ell+n+1).....(-m)]}{\left[\frac{1}{2\lambda_i} - \frac{1}{2\lambda_{i_1}}\right]^{m+n} \left[\frac{1}{2\lambda_i} - \frac{1}{2\lambda_{i_2}}\right]^{2m-\ell-n}} \tag{55}$$

where $i_1 = \text{modulo}_3(i) + 1$

$i_2 = \text{modulo}_3(i+1) + 1$

Finally, when the test inputs have the product multiplier, α, which is characterized by the Gamma distribution of Eq. (33), we take the expectation with respect to this variable and obtain

$$E_\alpha\left\{P^{(m)}_{D/FA}(\alpha)\right\} = \sum_{i=1}^{3} \sum_{\ell=1}^{m} A_{i\ell} E_\alpha\left\{P^{(m)}_{i\ell}\right\} \tag{56}$$

where

$$\begin{aligned}
E_\alpha\left\{P^{(m)}_{i\ell}\right\} &= E_\alpha\left\{G_{i\ell}(\alpha)\right\} && ; \quad \lambda_i > 0,\ c < 0 \\
E_\alpha\left\{P^{(m)}_{i\ell}\right\} &= 1 && ; \quad \lambda_i > 0,\ c > 0 \\
E_\alpha\left\{P^{(m)}_{i\ell}\right\} &= 1 - E_\alpha\left\{G_{i\ell}(\alpha)\right\} && ; \quad \lambda_i < 0,\ c > 0 \\
E_\alpha\left\{P^{(m)}_{i\ell}\right\} &= 0 && ; \quad \lambda_i < 0,\ c < 0
\end{aligned} \tag{57}$$

and

$$E_\alpha\{G_{i\ell}(\alpha)\} = \frac{1}{\bar{\alpha}^{\nu}\Gamma(\nu)} \sum_{k=0}^{\ell-1} \frac{\left(-\frac{C}{\lambda_i}\right)^{\nu+k}\left(\frac{\bar{\alpha}}{2}\right)^{\nu-k}}{2^{k-1}k!} K_{\nu-k}\left(2\sqrt{\frac{-C}{2\bar{\alpha}\lambda_i}}\right) \tag{58}$$

7.3 ANALYSIS OF THE PMF - GENERAL SOLUTION

Compared to the analysis of the OPD, discussed above, analysis of the matched filter algorithm is simpler because the algorithm is linear. We will briefly summarize here the solution for the multi-look case.

The output of the filter is a complex-Gaussian random variable comprised of the optimal weighted sum of the HH, HV, and VV data. This output is noncoherently detected and summed prior to being compared with the detection threshold T_D. Mathematically, the algorithm is represented as

$$y = \sum_{k=1}^{m} | \underline{h}^{\dagger} \underline{X}_k |^2 > T_D \tag{59}$$

Random variable y is chi-square, since it is the sum of m-independent exponential variables; therefore, in order to calculate the detection performance of the algorithm, we need only compute $E\{ | \underline{h}^{\dagger} \underline{X} |^2 \}$. We obtain

$$E\left\{ | \underline{h}^{\dagger} \underline{X} |^2 \right\} = \alpha d^2(\underline{h}) \tag{60}$$

where

$$d^2(\underline{h}) = \underline{h}^{\dagger} \Sigma \, \underline{h}$$

and α is the product multiplier

The conditional detection and false alarm probabilities, for a given value of the multiplier, α, are

$$P_{D/FA}^{(m)}(\alpha) = \sum_{k=0}^{m-1} \frac{\left(\dfrac{T_D}{\alpha \, d^2(\underline{h})} \right)^k}{k!} \exp \left\{ - \frac{T_D}{\alpha \, d^2(\underline{h})} \right\} \tag{61}$$

As with the OPD, the homogeneous target and clutter case is obtained by setting $\alpha = 1$ in the above expression.

When the product multiplier is modeled as a Gamma random variable with parameters $\{(\nu_i, \bar{\alpha}_i)\ i=t+c,c\}$, the average detection performance is calculated to be

$$E\{P_{D/FA}(\alpha)\} = \frac{2}{\bar{\alpha}\Gamma(\nu)} \sum_{k=0}^{m-1} \frac{(T_D/d^2(\underline{h}))^k}{k!} \left(\frac{T_D \, \bar{\alpha}}{d^2(\underline{h})} \right)^{(\nu-k)/2} K_{\nu-k}\left(2\sqrt{\frac{T_D}{d^2(h)\bar{\alpha}}} \right) \tag{62}$$

7.4 ANALYSIS OF SUBOPTIMAL DETECTORS

Two suboptimal polarimetric detectors which are under investigation use simpler detection statistics based on the polarimetric span ($|HH|^2 + 2|HV|^2 + |VV|^2$) and the single channel, $|HH|^2$. Analysis of each of these algorithms is a special case of a previous analysis. The single $|HH|^2$ channel detector is a special case of the matched filter. Its detection performance is evaluated by letting

$$\underline{h}^\dagger = (1 \quad 0 \quad 0) \tag{63}$$

in Equations (61) and (62).

Similarly, the detection statistic based on the polarimetric span is a special case of the OPD. Evaluation of its detection performance is easy because this detector is quadratic and of the form

$$y = \underline{X}^\dagger \begin{bmatrix} 1 & 0 & 0 \\ 0 & 2 & 0 \\ 0 & 0 & 1 \end{bmatrix} \underline{X} + C \quad > 0 \tag{64}$$

Thus, we modify Equation (40) to obtain the following:

$$\phi_{y/\alpha}(jw) = \int \cdots \int \exp\left\{ jw\underline{X}^\dagger \begin{bmatrix} 1 & 0 & 0 \\ 0 & 2 & 0 \\ 0 & 0 & 1 \end{bmatrix} \underline{X} + C \right\} \exp\left\{ \frac{-\underline{X}^\dagger \Sigma^{-1} \underline{X}}{\alpha} \right\} d\underline{X} \tag{65}$$

and use our previously developed solution to evaluate detection performance for this algorithm.

8. DUAL CHANNEL LL, LR DETECTION ALGORITHMS

Previous sections presented descriptions of detectors which used the full PSM (in a linear HH, HV, and VV polarization basis). An interesting alternative to the use of the full PSM for detection of targets has been proposed, namely dual channel LL, LR detection algorithms. In this scheme, left circular polarization is transmitted and both LL and LR polarizations are received simultaneously. As was done previously for algorithms using the full PSM, a number of algorithms for processing the LL and LR data will be discussed: (1) the optimal detector using both LL and LR data, (2) a matched filter detector using the LL and LR data, and (3) suboptimal detectors which use only the LL and LR power; one uses LL only, one LR only, and one sums the LL and LR power.

We describe the polarimetric feature vector comprised of the complex LL and LR returns by

$$\underline{Z} = \begin{bmatrix} LL_i + jLL_q \\ LR_i + jLR_q \end{bmatrix} = \begin{bmatrix} LL \\ LR \end{bmatrix} \tag{66}$$

Note that to be consistent with our previous definitions and for purposes of comparing results with the OPD, we express the LL and LR returns in terms of the linear basis by

$$\underline{Z} = T \begin{bmatrix} HH \\ HV \\ VV \end{bmatrix} \tag{67}$$

where

$$T = \begin{bmatrix} 0.5, & j, & -0.5 \\ 0.5j, & 0, & 0.5j \end{bmatrix}$$

From the polarization covariance matrix in the linear basis given by (3), the covariance matrix of $\underline{Z}$ is found to be

$$\Sigma_Z = \frac{\sigma}{4} \begin{bmatrix} 1-2\mathrm{Re}\{\rho\sqrt{\gamma}\}+\gamma+4\epsilon & 2\mathrm{Im}\{\rho\sqrt{\gamma}\}-j(1-\gamma) \\ 2\mathrm{Im}\{\rho\sqrt{\gamma}\}+j(1-\gamma) & 1+2\mathrm{Re}\{\rho\sqrt{\gamma}\}+\gamma \end{bmatrix} \tag{68}$$

The optimal detector using LL and LR data can be derived in the same manner as the OPD. That is, the optimal detector for LL and LR data, assuming that the feature vectors are jointly Gaussian with zero mean, is one which applies the test

$$\underline{Z}^{\dagger}\left(\Sigma_{Z_c}^{-1} - \Sigma_{Z_{t+c}}^{-1}\right)\underline{Z} + \ln \frac{\left|\Sigma_{Z_c}\right|}{\left|\Sigma_{Z_{t+c}}\right|} > \ln T_D \tag{69}$$

where $\Sigma_{Z_{t+c}}$ is the covariance matrix of the target-plus-clutter vector $\underline{Z}_{t+c}$, which is defined by

$$\underline{Z}_{t+c} = \underline{Z}_t + \underline{Z}_c \tag{70}$$

where

$$\Sigma_{Z_{t+c}} = \Sigma_{Z_t} + \Sigma_{Z_c} \tag{71}$$

The feature vectors $\underline{Z}$ comprised of LL and LR data are zero-mean and complex-Gaussian because they are obtained through the linear transformation (67) and because the feature vectors $\underline{X}$ comprised of HH, HV, and VV data were assumed to be zero-mean and complex-Gaussian.

The calculation of the performance of this detector, assuming the product target and clutter models described previously, is very similar to the calculation of the OPD. For the single-look case

$$P_{D/FA}(\alpha) = \sum_{i=1}^{2} A_i E\{P_i(\alpha)\} \tag{72}$$

where $E\{P_i(\alpha)\}$ is given by (50) where the eigenvalues (λ_1 λ_2) are obtained by the simultaneous diagonalization of $\left(\Sigma_{Z_c}^{-1} - \Sigma_{Z_{t+c}}^{-1}\right)$ and Σ_Z^{-1}, the covariance matrix of the test vector. For the multi-look case

$$E\left\{P_{D/FA}^{(m)}(\alpha)\right\} = \sum_{i=1}^{2} \sum_{\ell=1}^{m} A_{i\ell}\, E_\alpha\left\{P_{i\ell}^{(m)}\right\} \tag{73}$$

where $E_\alpha\left\{P_{i\ell}^{(m)}\right\}$ is given by (57) and (58) and

$$A_{i\ell} = \frac{(-2\lambda_i)^{\ell}}{(m-\ell)! \prod_{k=1}^{2} (-2\lambda_k)^m} \quad \frac{[-2m+\ell+1]\ [-2m+\ell+2]\cdots[-m]}{\left[\frac{1}{2\lambda_i} - \frac{1}{2\lambda_{i_1}}\right]^{2m-\ell}} \tag{74}$$

where $i_1 = \text{modulo}_2(i) + 1$

In Section 4, a polarimetric matched filter was derived using the full PSM. In a similar manner, a matched filter detector which optimizes the target-to-clutter ratio at the filter output can be defined using LL and LR data. As was shown for the detector using the PSM, the filter which maximizes T/C is the eigenvector which corresponds to the maximum eigenvalue of

$\left(\Sigma_{Z_c}^{-1} \Sigma_{Z_t}\right)$. The performance of the matched filter that uses LL and LR data can be calculated in the same fashion as for the matched filter that uses HH, HV, and VV data [see Equations (59) through (62)].

One suboptimal algorithm we studied calculates the sum of the powers in the LL and LR channels

$$y = |LL|^2 + |LR|^2 \tag{75}$$

Like the span detector, this algorithm is a suboptimal quadratic classifier since the detection statistic y can be obtained from

$$y = \begin{bmatrix} LL^* & LR^* \end{bmatrix} \begin{bmatrix} 1 & 0 \\ 0 & 1 \end{bmatrix} \begin{bmatrix} LL \\ LR \end{bmatrix} \tag{76}$$

The performance of this algorithm can be determined in the same manner as the performance of the span detector using the PSM.

Finally, since the LL and LR responses can be determined from a linear combination of the HH, HV, and VV returns as shown in Equation (67), the performance of the $|LL|$ only or $|LR|$ only detectors can also be determined using Equations (61) and (62).

9. ALGORITHM PERFORMANCE PREDICTIONS

The information presented in the previous sections includes the following: (1) a discussion of a number of detection algorithms, (2) development of homogeneous (Gaussian) and non-homogeneous (non-Gaussian) product target and clutter models, (3) derivations of the formulas necessary for evaluating the performance of various detectors for: single-look and multi-look cases, and for homogeneous and non-homogeneous targets and clutter. This section predicts the performance of the various detection algorithms in different situations. It does so by using parameters (σ, ϵ, γ, ρ) from measured target and clutter data to construct polarization covariance matrices of targets and clutter. These covariance matrices are used to calculate predicted detection performance of the various detectors. The subjects discussed in this section are

1. OPD, Span and $|HH|^2$ Performance Predictions
2. PMF Detection Performance Predictions
3. Detection Performance Using Circular Polarization
4. Discrimination Performance of the OPD

The performance predictions presented in this section of the report are based on polarimetric measurement data from typical ground targets and meadow clutter. Detection performance predictions presented in this section are for an armored target (target 1) versus clutter. Target discrimination results presented are for target 1 versus target 2 (a truck).

The polarimetric parameters of these targets and clutter are presented in Table I.

TABLE I

Polarimetric Parameters of Targets and Clutter

	σ	ϵ	γ	$\rho\sqrt{\gamma}$
TARGET 1	58.5	0.19	1.0	0.28
TARGET 2	618.3	0.02	1.1	0.83
CLUTTER	4.75	0.18	1.6	0.63

9.1 OPD, SPAN, AND $|HH|^2$ PERFORMANCE PREDICTIONS

This section compares performance predictions of three different detectors; (1) the optimal polarimetric detector (OPD) which uses all the information contained in the PSM, (2) the polarimetric span which uses the amplitude information but not the phase information in the PSM, and (3) the single-channel $|HH|^2$ detector which is the simplest radar detection scheme. This is the type of detector used in the HOWLS [1] program.

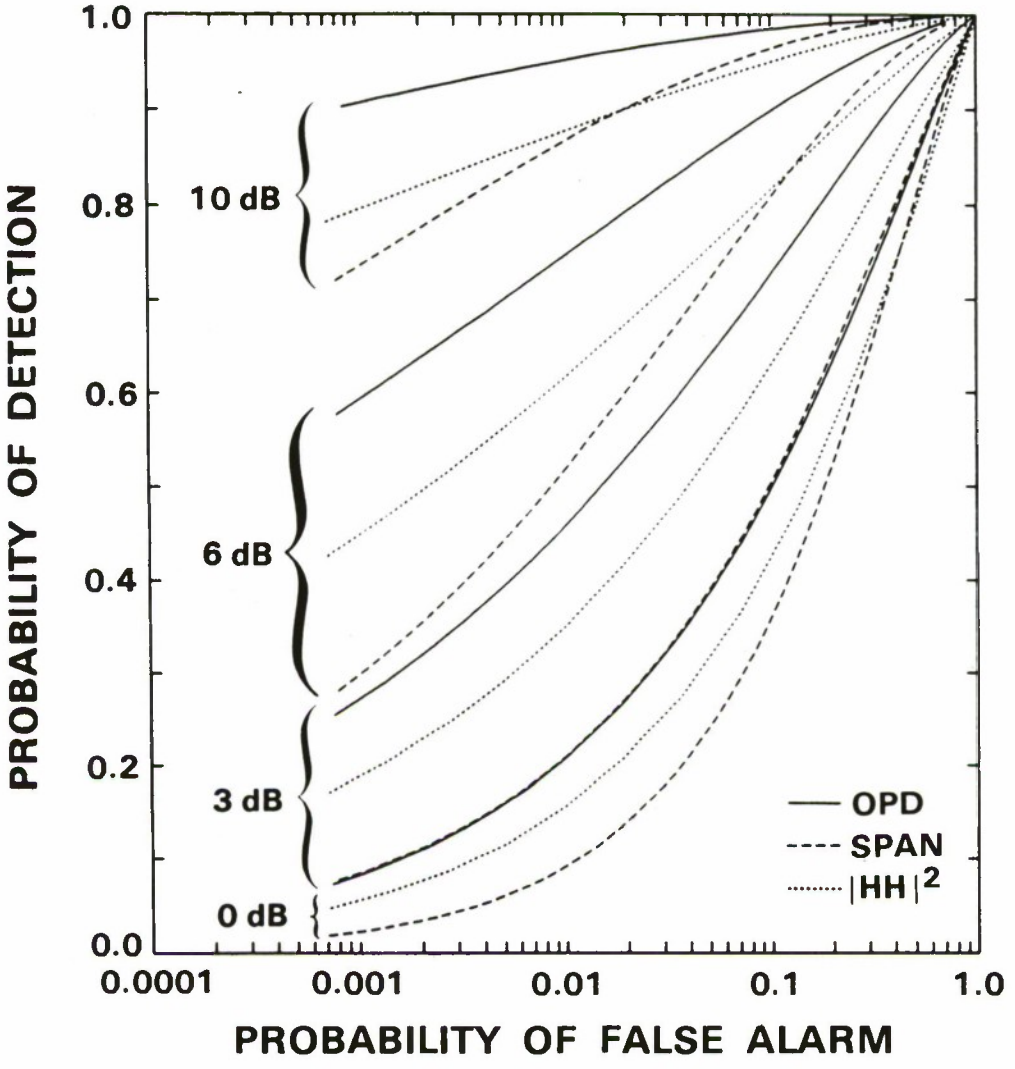

Figure 1. Algorithm performance comparison vs T/C ratio (single-look homogeneous models).

Single-Look Predictions: We have compared the performance of the OPD with the performance of both span and single-channel $|HH|^2$ algorithms. Both OPD and span processing require two pulses per look, whereas $|HH|^2$ processing requires only one. A fair comparison among the three algorithms requires the use of the same number of pulses. Therefore, we assumed that (1) the "extra" pulse for $|HH|^2$ processing would be used to provide a second, independent sample at a second frequency, and (2) the two independent $|HH|^2$ samples were noncoherently averaged.

For single-look processing with homogeneous targets and clutter, Figure 1 shows that the OPD outperformed span processing; this is to be expected, since the OPD uses all the polarimetric information in an optimally weighted fashion. The $|HH|^2$ processing also outperformed span processing, even though span processing uses all three polarimetric amplitudes; presumably this is due to the use of two independent samples in the $|HH|^2$ processing.

The OPD performed somewhat better than $|HH|^2$ processing. However, achievement of this improvement in detection performance requires exact knowledge of the target-to-clutter ratio as well as the target and clutter covariance statistics, since the optimal weighting coefficients are computed from this information. Since these target and clutter statistics are difficult to predict a priori, implementing the OPD in a real system would be difficult.

Contribution of Polarimetric Phase Information: The contribution of the polarimetric phase term, $|HH|\,|VV| \cos(\phi_{HH} - \phi_{VV})$, in target detection does not appear to be significant. In the first place, it can be shown that the distance measures of Equations (12)-(14) are dominated by the radar cross-section terms ($|HH|^2$, $|VV|^2$, $|HV|^2$). Another way to show this is to evaluate detection performance using amplitude-normalized feature vectors. The optimal processor of normalized data (OPDN) [17] provides the best possible performance for normalized Gaussian feature vectors. The optimal performance for the normalized data is shown in the curves of Figure 2. A comparison of the performance of the optimal processor for normalized data (Figure 2) with that of the OPD which processes unnormalized data (Figure 1) clearly shows that it is the polarimetric amplitude information which provides the good detection performance results of the OPD.

Multi-Look Processing: Figure 3 summarizes the performance predictions for the 6-dB target-to-clutter ratio case using multi-look processing for homogeneous targets and clutter. $|HH|^2$ detection performance is again superior to detection using the span statistic. An optimally weighted combination of the $|HH|^2$, $|VV|^2$ and $|HV|^2$ amplitudes might improve performance of the span detector somewhat; however, the span performance is bounded above by the OPD, and HH processing is not significantly worse than OPD performance.

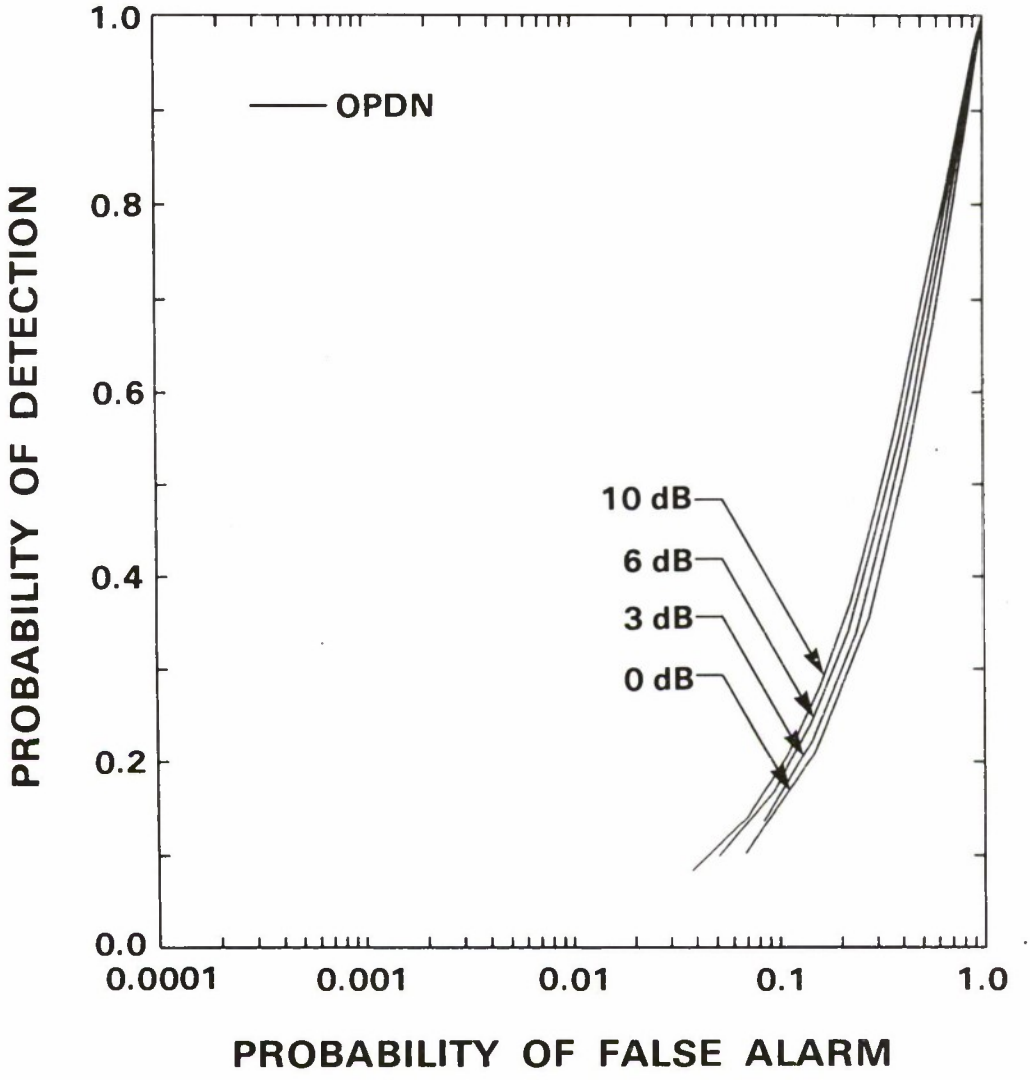

Figure 2. Performance of optimal normalized polarimetric detector vs T/C ratio (single-look, homogeneous models).

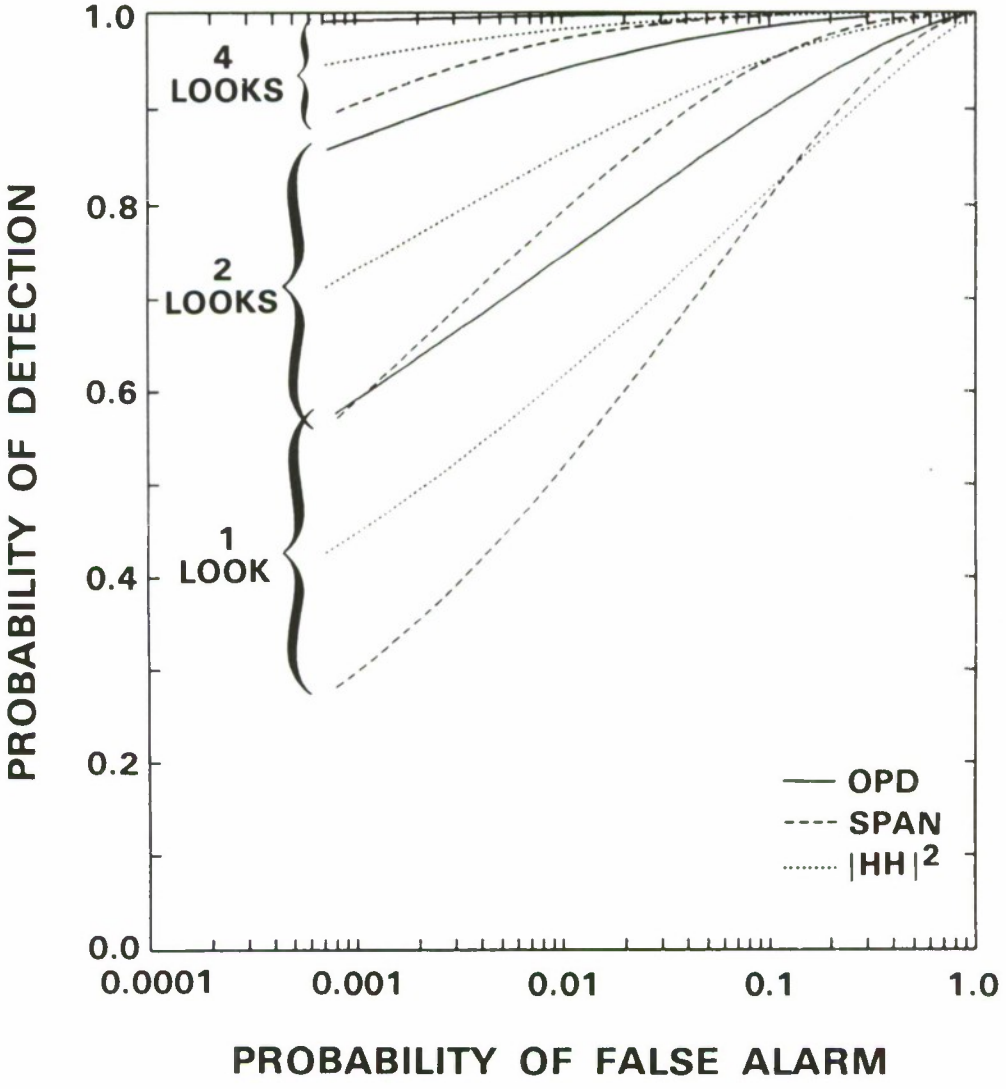

103872-2

Figure 3. Algorithm performance comparison vs N looks (T/C = 6 dB, homogeneous models).

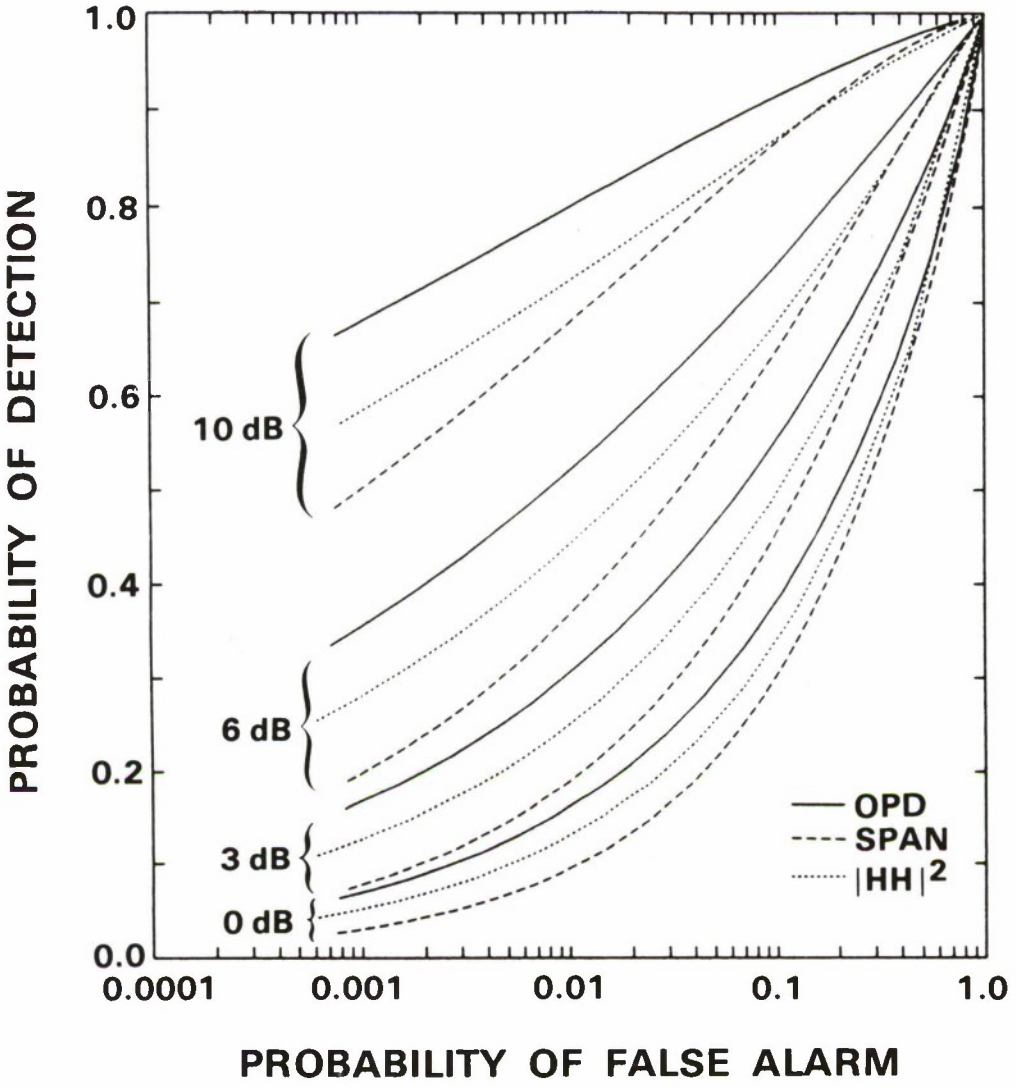

103872-3

Figure 4. Algorithm performance comparison vs T/C ratio [single-look product model (α_t = 3 dB, α_c = 1.5 dB)].

Product Model Effects: The results of Figure 3, which correspond to multi-look processing of statistically independent PSM samples, are very optimistic because idealized homogeneous target and clutter models were used. With more realistic product model representations of targets and clutter, we obtain performance results for HH processing which are consistent with those achieved using the HOWLS [1] radar data.

The curves of Figures 4 and 5 show more realistic algorithm performance predictions based on the product target and clutter models. These figures show the performance of the OPD designed for homogeneous target and clutter models but tested against nonhomogeneous product target and clutter model inputs. Comparing Figure 4 with Figure 1 (and Figure 5 with Figure 3) shows the deleterious effect of nonhomogeneous targets and clutter on the performance of all three algorithms. For example, for $P_{FA} = 10^{-3}$ the detection performance of the OPD with 10-dB target-to-clutter ratio is degraded from 90 percent to less than 70 percent. Similar reductions can be observed for the other algorithms and at other target-to-clutter ratios.

Furthermore, the performance improvement achieved through multi-look processing is considerably reduced when the more realistic (nonhomogeneous) target and clutter models are used (compare Figure 5 with Figure 3). Thus, the benefits of frequency averaging of independent PSM samples are reduced due to nonhomogeneity of the target and clutter models. These observations are consistent with results obtained previously using HOWLS data [1]. Also, the performance advantage of the OPD relative to $|HH|^2$ processing is reduced in this case since the OPD detector was designed to be optimal for homogeneous target and clutter models.

Sensitivity to Product Model Parameters: In a previous study [1], we showed that the nonhomogeneity of ground clutter and aspect angle variability of targets were dominant factors in the reduction of detection performance of a single-channel $|HH|^2$ detector; that is, the sensitivity of detection performance to the target and clutter parameters, α_t and α_c, is quite severe. To verify that this effect also applies to polarimetric detection algorithms we have evaluated the performance of the OPD over a reasonable range of α_c (1, 1.5, 2, 2.5, and 3 dB). Figure 6 shows the OPD performance predictions for single-look and 4-look processing. The top curves (denoted as $\alpha_c = -\infty$) correspond to the homogeneous clutter model and are included as an upper bound on performance. From the curves, it is clear that detection performance is degraded rapidly with the increasing nonhomogeneity of clutter.

We have also evaluated the performance of the OPD over a reasonable range of α_t (1, 2, 3, and 4 dB). Figure 7 shows the resulting performance predictions. From these curves, it is seen that the single-look results are less affected by a change in α_t than the 4-look results. Nevertheless, there is, in general, a fairly strong dependence on α_t.

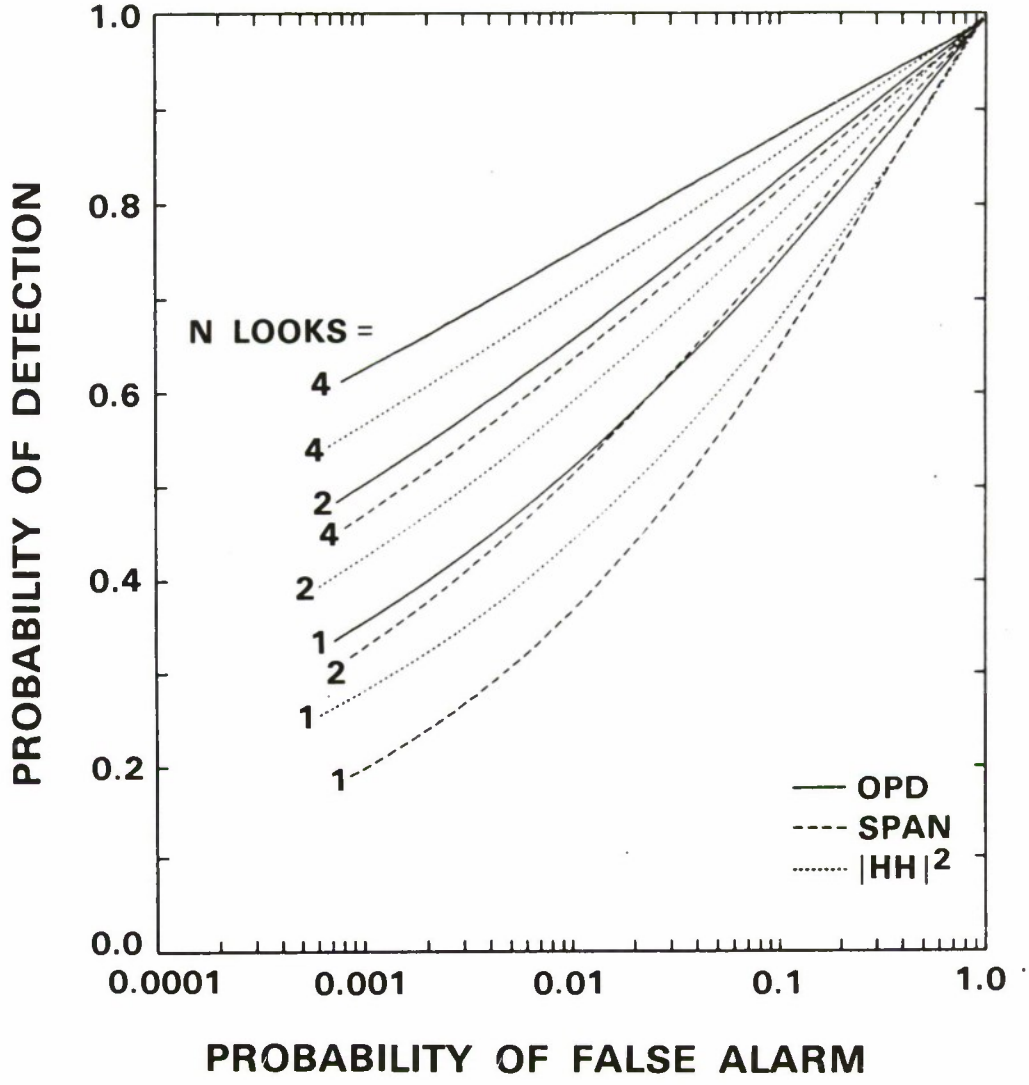

103872-4

Figure 5. Algorithm performance comparison vs N looks [T/C = 6 dB, product models (α_t = 3 dB, α_c = 1.5 dB)].

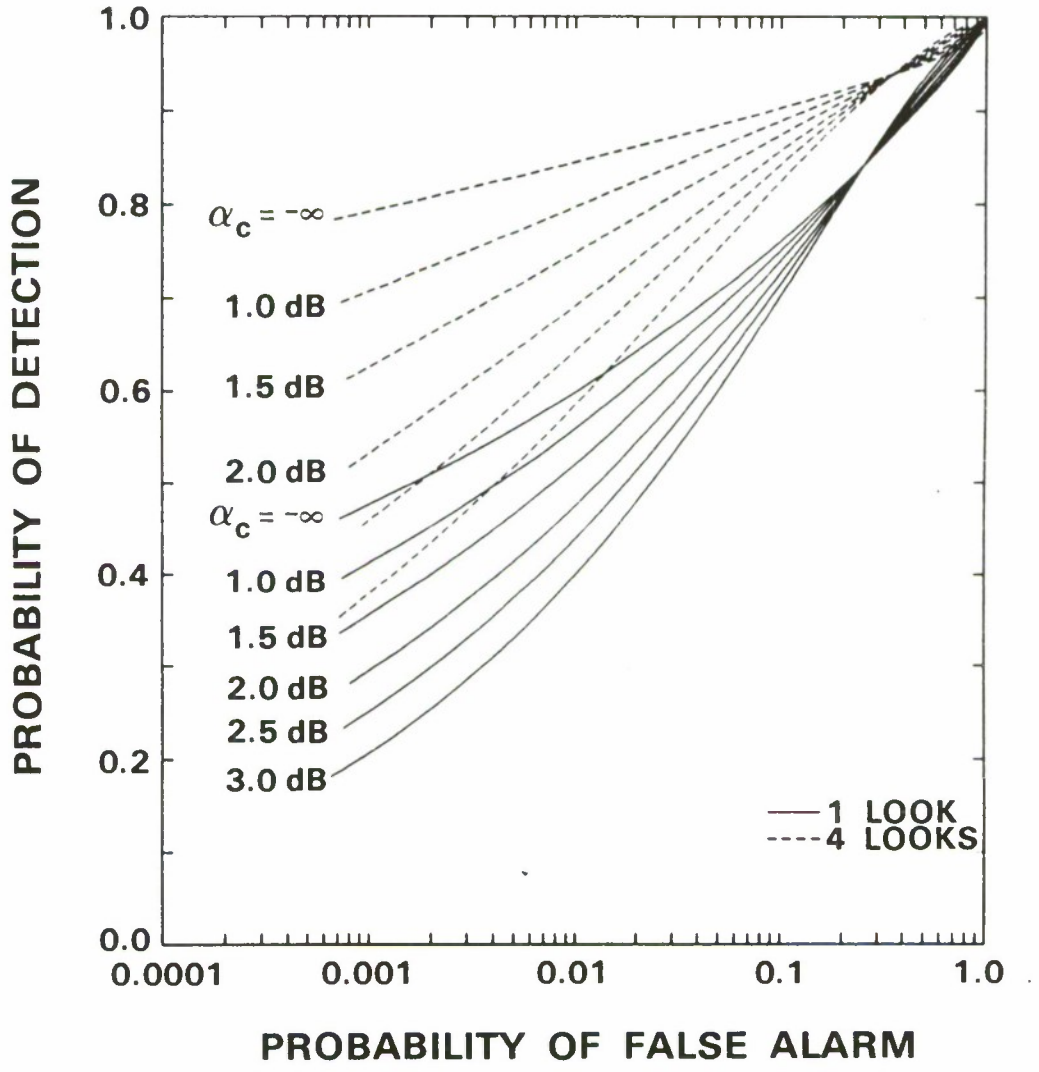

103206-1

Figure 6. Sensitivity of OPD to clutter St. Dev. [T/C = 6 dB, product model (α_t = 3 dB)].

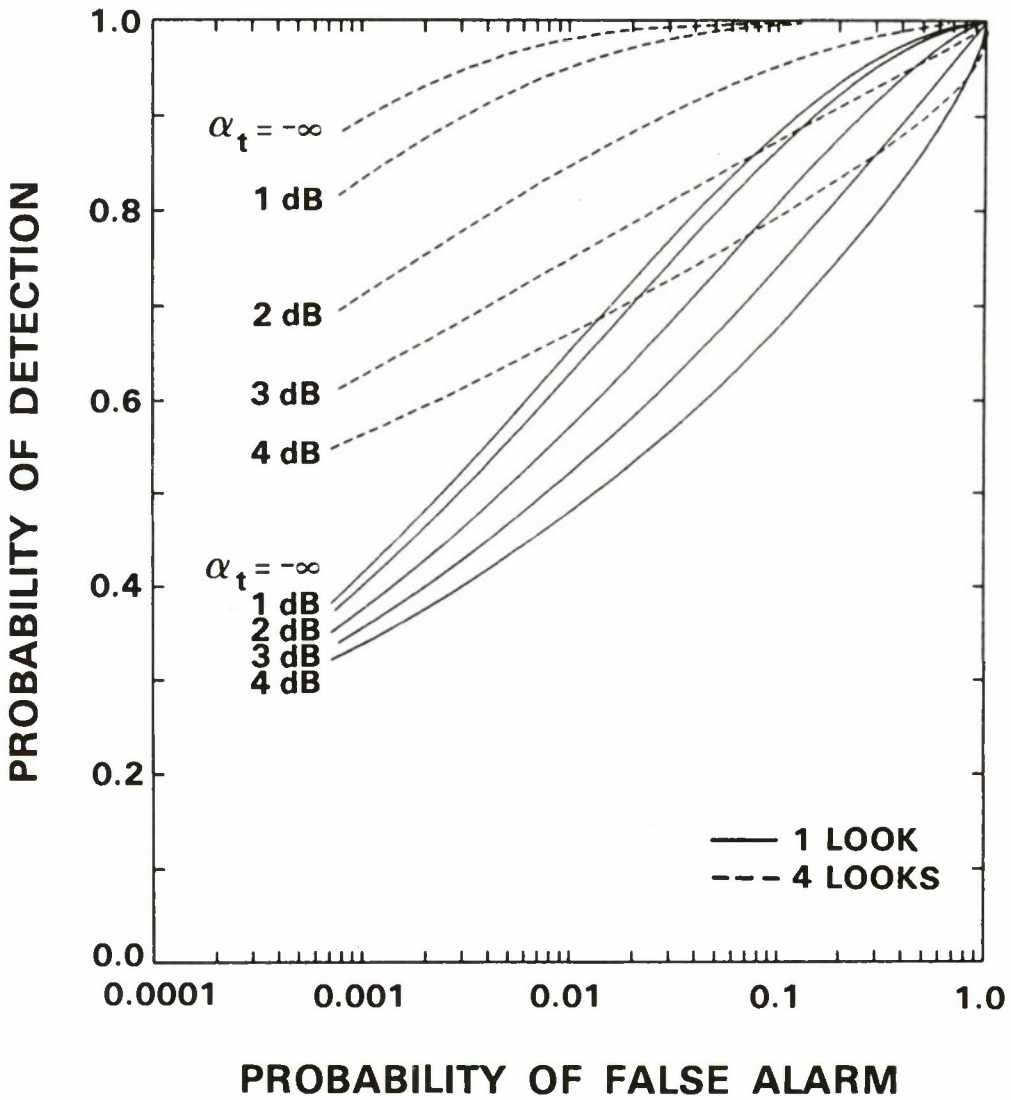

103206-2

Figure 7. Sensitivity of OPD to target St. Dev. [T/C = 6 dB, product model (α_c = 1.5 dB)].

Comparison of OPD with Product-Model Likelihood Ratio Test: The product-model likelihood ratio test is the optimal detector for product-model targets and clutter. This algorithm was defined in Equation (37). Since the OPD (designed for homogeneous models) exhibits degraded performance when tested with nonhomogeneous models, it is of interest to compare the performance of the OPD with that of the LRT algorithm. Our studies indicate that over the range of parameter variations of interest the OPD performs almost as well as the LRT algorithm.

9.2 PMF DETECTION PERFORMANCE PREDICTIONS

The OPD discussed in previous sections is the optimal processor assuming Gaussian statistics; however, it is nonlinear, and requires a priori knowledge of both the target and clutter covariances and the target-to-clutter ratio. The PMF on the other hand is a linear processor which also requires a priori knowledge of the target and clutter covariances. However, the PMF (a constant-coefficient filter) does not require a priori knowledge of the target-to-clutter ratio.

This section presents the results of our polarimetric matched filter studies. We designed the PMF based on the target and clutter covariances specified earlier [see Equations (18)-(23)]. Evaluating the eigenvalues and eigenvectors of the matrix $\Sigma_c \Sigma_t$, yields the following solutions:

$$\text{(i)} \quad \lambda_1 = 12.78 \leftrightarrow \underline{h}_1 = \begin{bmatrix} 0 \\ 1 \\ 0 \end{bmatrix}$$

$$\text{(ii)} \quad \lambda_2 = 7.54 \leftrightarrow \underline{h}_2 = \begin{bmatrix} 1 \\ 0 \\ 3.6 \end{bmatrix}$$

$$\text{(iii)} \quad \lambda_3 = 15.58 \leftrightarrow \underline{h}_3 = \begin{bmatrix} 1 \\ 0 \\ -0.5 \end{bmatrix}$$

The best PMF is, therefore, specified by solution (iii) above. We have compared the detection performance of this PMF with that of the single-channel $|HH|^2$ detector. One of our objectives was to make a direct comparison of the PMF with the results of the HOWLS radar [1], so for these comparisons we have used product target and clutter models with parameters α_t = 3 dB, α_c = 2 dB and (T/C) = 6 dB. Equations (61) and (62) were used to obtain the performance predictions. Figure 8 summarizes the results, showing detection performance of the PMF with 1, 2, 4, 8, and 16 independent polarimetric samples processed. Since these polarimetric samples require transmitting 2, 4, 8, 16, and 32 radar pulses, we show the comparison with $|HH|^2$ processing using these same numbers of transmitted pulses.

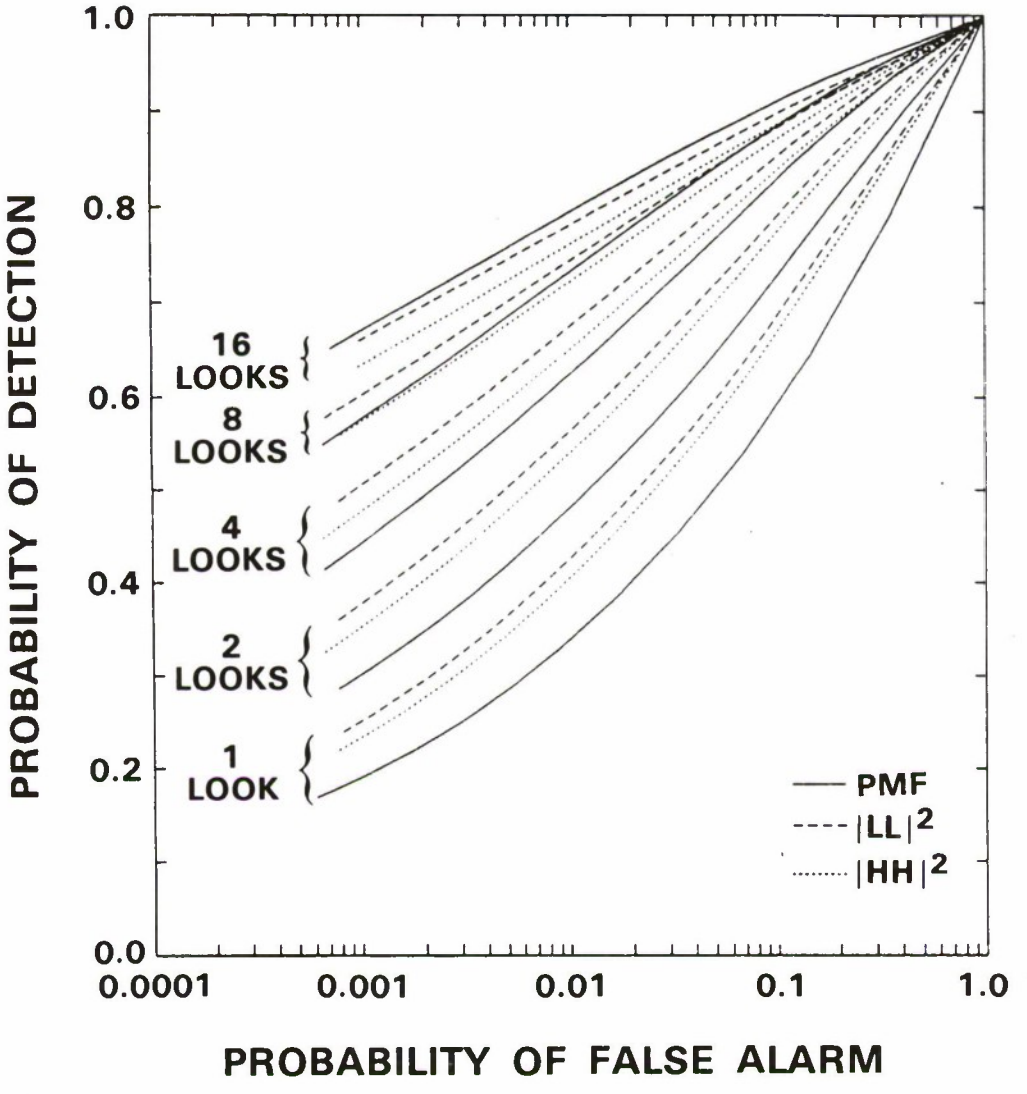

103872-5

Figure 8. Algorithm performance comparison [T/C = 6 dB, product models (α_t = 3 dB, α_c = 2 dB)].

The PMF (with an equivalent number of transmitted pulses) does not perform as well as $|HH|^2$ processing until we process about 8 independent fully polarimetric measurements. With 8 independent looks (16 pulses transmitted) the two algorithms provide essentially the same performance. The performance predictions with 16 pulses transmitted agree closely with the HOWLS measurements (i.e., $P_D \sim 50$ percent and $P_{FA} \sim 10^{-3}$ with 6 dB target-to-clutter ratio). As more independent looks are processed, the PMF begins to outperform the $|HH|^2$ detector.

We have also made a performance comparison of the best PMF design with a detector using a circular transmit, circular receive $|LL|^2$ system. It has been reported that this algorithm achieves a better target-to-clutter ratio than the linear transmit, linear receive $|HH|^2$ system. This is true because the even bounce $|LL|^2$ clutter return is less than the $|HH|^2$ clutter return, whereas the even bounce $|LL|^2$ target return is about the same as the $|HH|^2$ target return. Also, a single $|LL|^2$ measurement requires only 1 pulse transmission. Figure 8 shows that the even channel $|LL|^2$ detection performance is slightly better than the $|HH|^2$ detection performance. All three detectors are essentially equivalent in performance with 16 pulses transmitted.

9.3 DETECTION PERFORMANCE USING CIRCULAR POLARIZATION

The performance of the algorithms which use $|LL|^2$ only and $|HH|^2$ only (see Figure 8) indicated that the two polarizations necessary to construct the full PSM for purposes of implementing the OPD or the PMF may not improve detection performance significantly. Therefore, in this section we examine the performance of detection algorithms that use circularly polarized data. All of the detectors we study use a single circular transmit polarization. Specifically, the detection algorithms we examine are: (1) the optimal quadratic detector using complex LL and LR data, (2) a detector using the sum of the powers $|LL|^2 + |LR|^2$, (3) a matched filter using complex LL, LR data, and (4) detectors using either $|LL|^2$ or $|LR|^2$ data.

The curves in Figure 9 compare the results using the OPD, the optimal quadratic detector using complex LL and LR data, and the suboptimal detector which uses the sum of the powers $|LL|^2 + |LR|^2$, for the situation where two pulses are transmitted (which is the minimum required by the OPD). The analysis used product-model target and clutter inputs. Figure 9 shows performance predictions versus target-to-clutter ratio. Figure 10 shows the detection performance of these same algorithms for a fixed target-to-clutter ratio of 6 dB, for 1-, 2-, and 4-look data, where each look consists of two transmitted pulses. These figures show that optimal processing of two independent measurements of complex LL, LR data provides better detection performance than the OPD (which requires two pulses to construct the PSM). They also show that the $|LL|^2 + |LR|^2$ detector (which, unlike the other two algorithms, requires no previous information concerning the target and clutter covariances or the target-to-clutter ratio) provides performance comparable to that of the OPD.

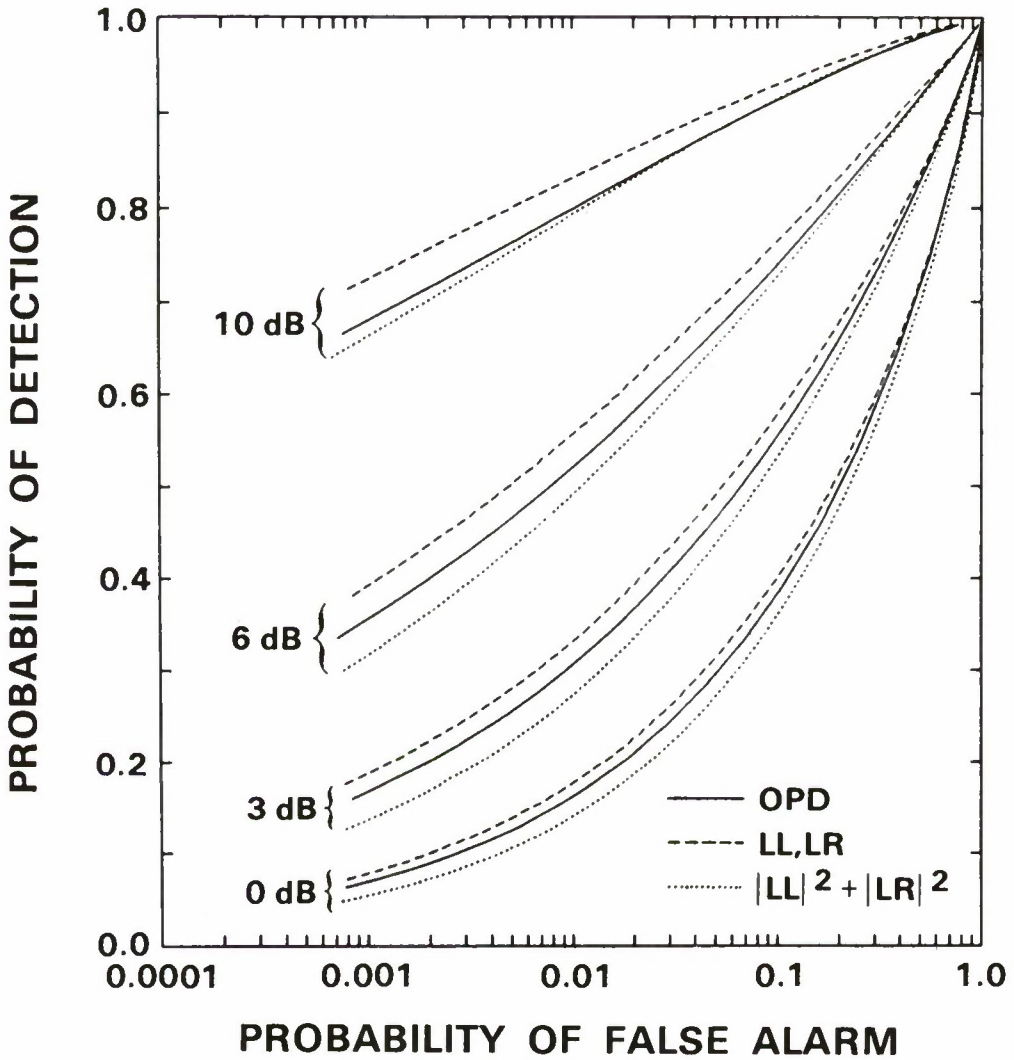

Figure 9. Algorithm performance comparison vs T/C ratio [single-look product model (α_t = 3 dB, α_c = 1.5 dB)].

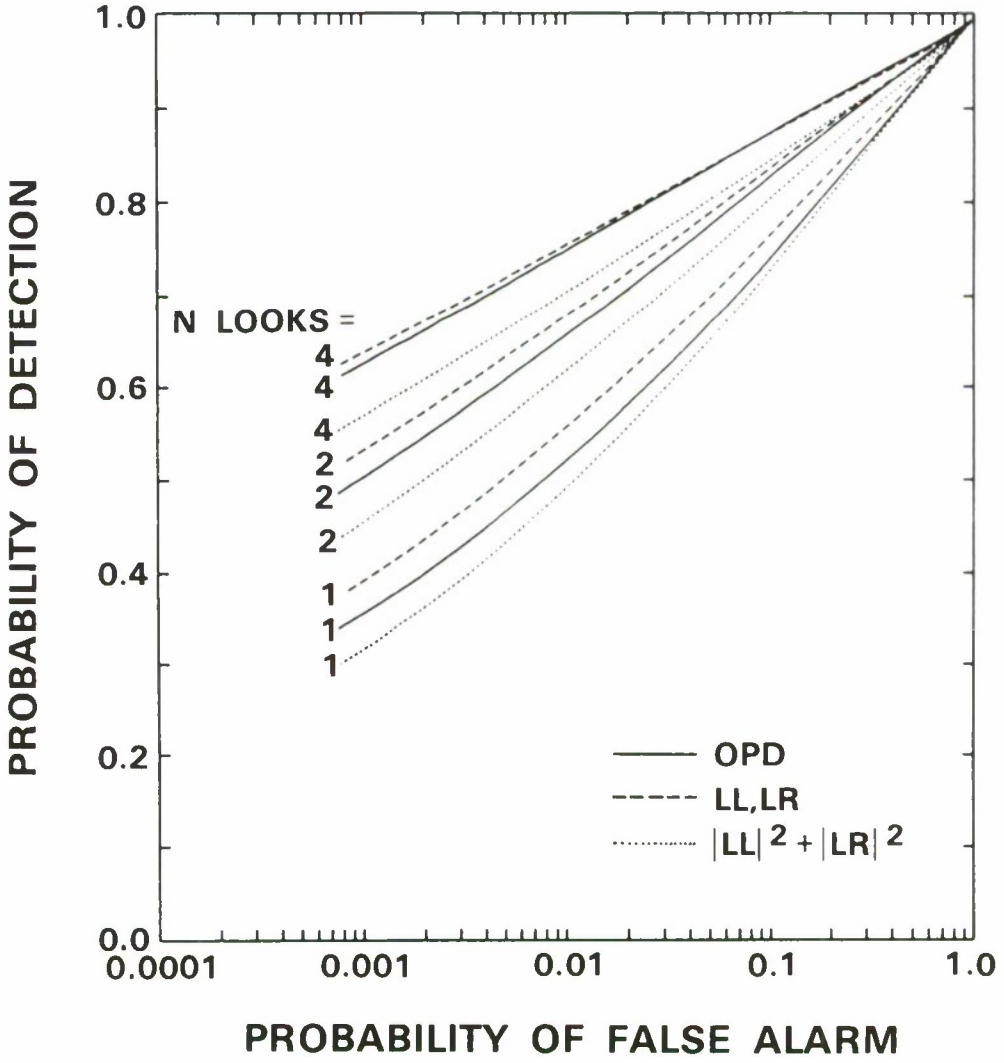

103206-4

Figure 10. Algorithm performance comparison vs N looks [T/C = 6 dB, product models (α_t = 3 dB, α_c = 1.5 dB)].

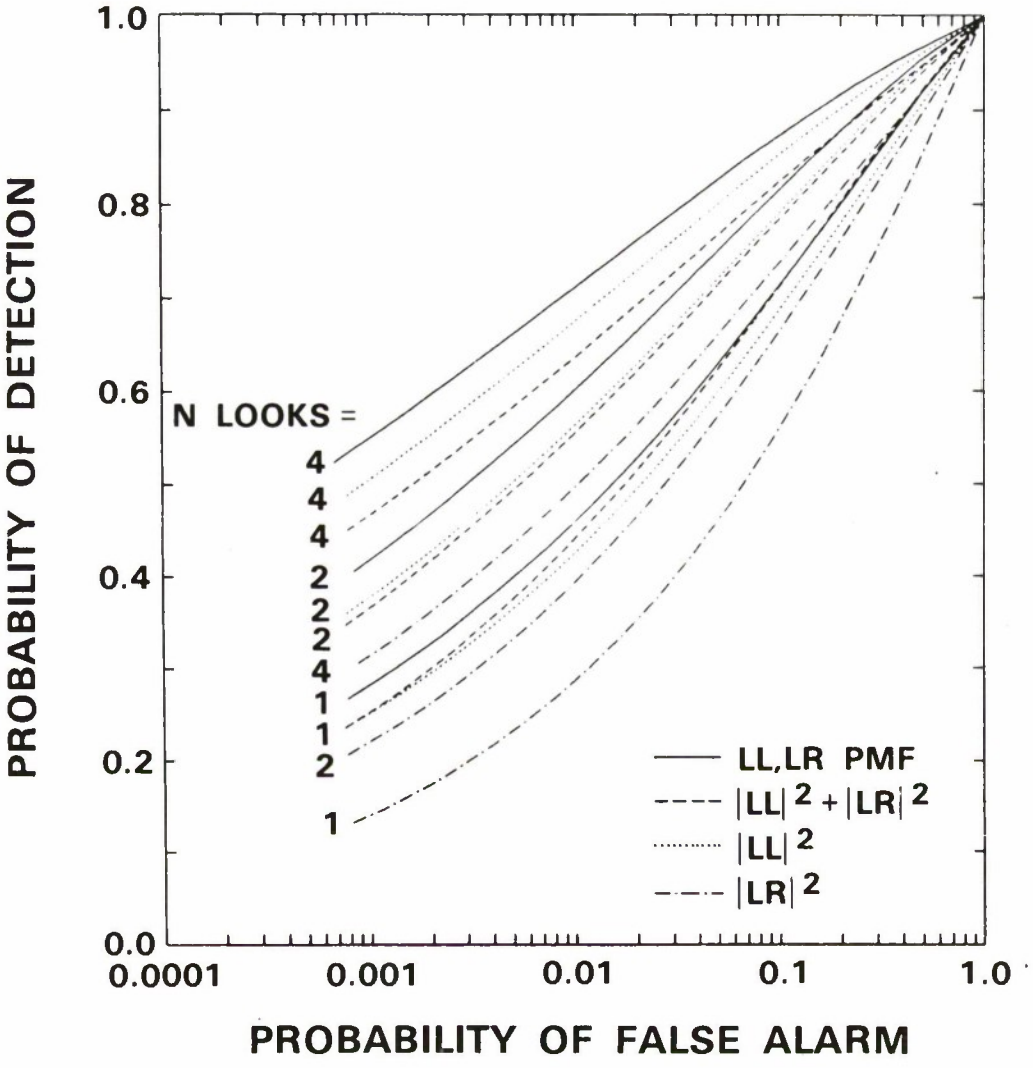

Figure 11. Algorithm performance comparison [T/C = 6 dB, product models (α_t = 3 dB, α_c = 2 dB)].

Figure 11 compares the performance of four detection algorithms which require only one transmit pulse per look: (1) the LL, LR matched filter, (2) the $|LL|^2 + |LR|^2$ detector, (3) the $|LL|^2$ only detector, and (4) the $|LR|^2$ only detector. These curves indicate that the performance of the $|LL|^2$ channel-only detector compares well with that of the matched filter detector (which requires a priori knowledge of the target and clutter covariances). The $|LL|^2$ channel-only detector provides much better performance than the $|LR|^2$ channel-only detector. Not surprisingly, the $|LL|^2$ channel detector is also superior to the $|LL|^2 + |LR|^2$ detector (because the two channels are simply added without optimum weighting). Figure 11 shows that the best combination of polarization channels to use in a detector is dependent on the statistics (i.e., covariance matrices) of the particular target and clutter under study (recall that all the figures show results of detection studies of an armored target versus meadow clutter). The relative performance of the detectors shown in Figure 11 might be different for different targets and/or clutter types. Obviously, the best combination of polarization channels is highly dependent on the covariance matrices of target and clutter.

9.4 DISCRIMINATION PERFORMANCE OF THE OPD

Once a target has been detected, it may be important to discriminate between different target types (e.g., tank versus truck). The collected polarimetric data for various targets may contain information as to the type of target being observed, which may be used by a polarimetric classifier to achieve discrimination. This section presents the results of studies which used the OPD as a polarimetric classifier.

In our discrimination studies, we used normalized feature vectors having unit length. This has the advantage of removing the product scale factor from the data, so that classifier design becomes independent of absolute radar cross-section. Only the relative amplitude differences between the complex HH, HV, and VV elements, and the polarimetric phase $\phi_{HH} - \phi_{VV}$, are used to discriminate among target types. Table II shows the average probability of classification error for the armored target versus the truck. The table includes results for various numbers of looks (i.e., various numbers of independent polarimetric measurements processed) and for target-to-clutter ratios of 0, 3, 6, and 10 dB for target 1 versus clutter. In each case, the target-to-clutter ratio for target 2 versus clutter is 10 dB higher due to the larger radar cross section of target 2 (see Table I).

Table II shows the average probability of classification error for the armored target versus the truck.

TABLE II

Probability of Classification Error (%)

T/C Ratio	Number of Looks 1	2	4	8
10 dB	24.6	17.6	10.6	5.2
6 dB	26.0	19.2	12.0	6.2
3 dB	27.8	21.0	14.0	7.4
0 dB	30.2	24.3	17.1	10.0

The results shown in Table II suggest that polarimetric information is useful in discriminating between target types. However, to achieve reliable performance requires multi-look processing with reasonably high (6-10 dB) target-to-clutter ratios. Also, good discrimination can only be achieved for targets exhibiting discernible differences in polarization characteristics (e.g., the values seen for ϵ and ρ in Table I).

It might be possible to separate these two specific targets on the basis of absolute radar cross-section (RCS) only. However, absolute radar cross-section is not used in this classifier because (1) RCS can be easily modified, and (2) to use absolute RCS would require very accurate absolute calibration of the test data with respect to the training data. The normalized polarimetric classifier does make use of the relative amplitudes in the HH, HV, and VV channels.

10. SUMMARY

This report summarizes a study of target detection algorithms which use polarimetric radar data. A model which accounts for the spatial nonhomogeneity of ground clutter and the aspect angle variability of targets was developed and the performance of various algorithms evaluated.

Our study found that the additional information provided by the full PSM measurement, even when processed in an optimal fashion, does not aid significantly in target detection. That is, a radar which transmits and receives a single polarization (e.g., HH or LL) will obtain almost as good performance as one which measures the full PSM. Also, to achieve the additional performance improvement from the OPD (which uses the full PSM), one must have exact knowledge of the target and clutter covariances, as well as the target-to-clutter ratio. When these covariances are not known, the single-polarimetric-channel detector provides the best performance. Therefore, independent, multi-look, single-polarization algorithms appear to be the best approach to target detection.

Our studies showed that when a single polarization is used, $|LL|^2$ (even bounce) circular polarization provides slightly better performance than $|HH|^2$ (linear) polarization. However, the clutter data base used in these studies was limited, and further study of this problem using various types of clutter (for example, snow clutter) will be necessary.

Once a target is detected, information contained in the PSM may be useful for discriminating between target types (e.g., armored target versus truck). Our preliminary results indicate that, for discrimination to be effective, many independent looks at the target are required and the target-to-clutter ratio must be fairly high. This area will require further study using a variety of target types.

Another area in need of further investigation is the development of more realistic statistical target models. Some targets have different polarimetric properties at different aspect angles. Thus a more realistic statistical target model would be one which uses different covariance matrices to characterize a target at different aspect angles.

ACKNOWLEDGMENTS

The authors would like to thank their colleagues, Mitchell I. Mirkin, who provided help with the polarimetric clutter model and Richard M. Barnes, who assisted with the detection theory and fundamental concepts in polarimetry; Steven M. Auerbach, who edited the report; and the group leader, Gerald B. Morse, for his help and encouragement.

REFERENCES

1. V.L. Lynn, "HOWLS Radar Development," Millimeter Wave Radar, Ed. Stephen L. Johnson (Artech House, Inc, Dedham, MA, 1980).

2. L.M. Novak and F.W. Vote, "Millimeter Airborne Radar Target Detection and Selection Techniques," Proc. NAECON 1979 Conference, Dayton, OH, 15-17 May 1979.

3. R. Shin, L.M. Novak, and M. Borgeaud, "Theoretical Models for Polarimetric Radar Clutter," Proc. 10th DARPA MMW/Tri-Service Symposium, Adelphi, MD, 8-10 April 1986.

4. R.M. Barnes, "Detection of a Randomly Polarized Target," PhD Thesis, Northeastern University, Department of Electrical Engineering (June 1984).

5. K. Fukunaga, Introduction to Statistical Pattern Recognition (Academic Press, New York, 1972).

6. J. Kong, A. Swartz, H. Yueh, L.M. Novak, and R. Shin, "Identification of Terrain Cover Using the Optimal Polarimetric Classifier," J. Electromagn. Waves Appl. Vol. 2, No. 2 (1988).

7. J. Cadzow, "Generalized Digital Matched Filtering," Proc. 12th Southeastern Symposium on System Theory," Virginia Beach, VA, 19-20 May 1980.

8. E. Jakeman and P. Pusey, "A Model for Non-Rayleigh Sea Clutter," IEEE. Trans. Antennas Propag. (November 1976).

9. D. Lewinski, "Nonstationary Probabilistic Target and Clutter Scattering Models," IEEE Trans. Antennas Propag. (May 1983).

10. J. Jao, "Amplitude Distribution of Composite Terrain Clutter and the K-Distribution," IEEE Trans. Antennas Propag. (October 1984).

11. I. Gradsteyn and I. Rhzhik, Table of Integrals, Series, and Products (Academic Press, New York, 1980).

12. K. Fukunaga and T. Krile, "Calculation of Bayes Recognition Error for Two Multivariate Gaussian Distributions," IEEE Trans. Comput. (March 1969).

13. L.M. Novak, "On the Sensitivity of Bayes and Fisher Classifiers in Radar Target Detection," Proc. 18th Asilomar Conference on Circuits, Systems, and Computers, Pacific Grove, CA, November 1984.

14. MACSYMA Reference Manual, Vol. 1, M.I.T., Cambridge, MA, 1983.

15. L.M. Novak and M.B. Sechtin, "On the Performance of Linear and Quadratic Classifiers in Radar Target Detection," Proc. 20th Asilomar Conference on Circuits, Systems, and Computers, Pacific Grove, CA, November 1986.

16. A. Oppenheim and A. Willsky, Signals and Systems (Prentice Hall, New Jersey, 1983), p. 772.

17. H. Yueh, A. Swartz, J. Kong, R. Shin, and L.M. Novak, "Bayes Classification of Terrain Cover Using Normalized Polarimetric Data," to appear in Journal of Geophysical Research.

APPENDIX

This appendix provides the solution for the calculation of the eigenvalues of the matrix product $\Sigma_3(\Sigma_1^{-1} - \Sigma_2^{-1})$. Equivalently, we may simultaneously diagonalize the following two matrices:

$$\Sigma_1^{-1} - \Sigma_2^{-1} \longrightarrow \Lambda \tag{A-1}$$

$$\Sigma_3^{-1} \longrightarrow I \tag{A-2}$$

When this is done, the diagonal elements of the matrix Λ are the desired eigenvalues. These eigenvalues are required in the performance evaluation of the optimal polarimetric detector. In this appendix, we assume the polarimetric measurement vector to be a real, 6-dimensional zero-mean, Gaussian vector

$$\underline{X} = (HH_I,\ HH_Q,\ HV_I,\ HV_Q,\ VV_I,\ VV_Q)' \tag{A-3}$$

with real 6 x 6 covariances Σ_1, Σ_2, Σ_3 of the form

$$\Sigma_i = \frac{\sigma_{HH}}{2} \left[\begin{array}{cc|cc|cc} 1 & 0 & 0 & 0 & \sqrt{\gamma}\mathrm{Re}(\rho) & -\sqrt{\gamma}\mathrm{Im}(\rho) \\ 0 & 1 & 0 & 0 & \sqrt{\gamma}\mathrm{Im}(\rho) & \sqrt{\gamma}\mathrm{Re}(\rho) \\ \hline 0 & 0 & \epsilon & 0 & 0 & 0 \\ 0 & 0 & 0 & \epsilon & 0 & 0 \\ \hline \sqrt{\gamma}\mathrm{Re}(\rho) & \sqrt{\gamma}\mathrm{Im}(\rho) & 0 & 0 & \gamma & 0 \\ -\sqrt{\gamma}\mathrm{Im}(\rho) & \sqrt{\gamma}\mathrm{Re}(\rho) & 0 & 0 & 0 & \gamma \end{array}\right] ; \quad i=1,2,3 \tag{A-4}$$

This solution is general in that we have assumed the correlation parameter, ρ, to be complex. The real 6 x 6 matrix has 3 eigenvalues, each of multiplicity two. We present the analytical solution for these eigenvalues λ_1, λ_2, λ_3 in the following FORTRAN subroutine.

```
      subroutine eigvals(e1,g1,r1,s1,e2,g2,r2,s2,e3,g3,r3,s3)

c-----------------------------------------------------------------------
c
c       This program generates the eigenvalues of an input matrix in
c       the form (sigma.3)x(sigma.1.inverse - sigma.2.inverse) where
c       sigma.1, sigma.2, and sigma.3 are all 6x6 covariance matrices
c       whose elements are determined by the parameters contained in
c       the input data file.  The equations for the eigenvalues were
c       obtained using MACSYMA.
c
c-----------------------------------------------------------------------

      parameter(inlu=12,outlu=21)

c     DATA STRUCTURES
      double precision e1,e2,g1,g2,s1,s2
      double precision l1,l2,l3,l4,l5,l6,lam(3)
      double precision a1,a2,a3,b1,b2,b3,den1,den2
      double precision e3,g3,s3
      complex*16 r1,r2,r3

c     CHARACTER STRINGS
      character*50 infil,filname,gettext

c-----------------------------------------------------------------------

      a1=(g1**0.5)*dreal(r1)
      b1=(g1**0.5)*dimag(r1)
      a2=(g2**0.5)*dreal(r2)
      b2=(g2**0.5)*dimag(r2)
      a3=(g3**0.5)*dreal(r3)
      b3=(g3**0.5)*dimag(r3)

      den1=(g1-(b1**2)-(a1**2))*s1
      den2=(g2-(b2**2)-(a2**2))*s2

      x=(g1/den1)-(g2/den2)
      y=(a2/den2)-(a1/den1)
      z=(b2/den2)-(b1/den1)
      v=(1/den1)-(1/den2)
      w=(1/(e1*s1))-(1/(e2*s2))

c------Compute the eigenvalues of the matrix
c       (sigma.3) x (sigma.1.inverse - sigma.2.inverse)

      l1=(s3*(x-sqrt(g3*(4*z**2+4*y**2-2*v*x)+a3**2*(4*v*x-4*z**2)+a3*
     1   (8*b3*y*z+4*x*y+4*g3*v*y)+b3*(4*x*z+4*g3*v*z)+b3**2*(4*v*x-4*
     2   y**2)+x**2+g3**2*v**2))+2*b3*s3*z+2*a3*s3*y+g3*s3*v)/2.0


      l2=(s3*(sqrt(g3*(4*z**2+4*y**2-2*v*x)+a3**2*(4*v*x-4*z**2)+a3*
     1   (8*b3*y*z+4*x*y+4*g3*v*y)+b3*(4*x*z+4*g3*v*z)+b3**2*(4*v*x-4*
     2   y**2)+x**2+g3**2*v**2)+x)+2*b3*s3*z+2*a3*s3*y+g3*s3*v)/2.0

      l3=e3*s3*w

      lam(1)=l1
      lam(2)=l2
      lam(3)=l3
```

REPORT DOCUMENTATION PAGE

1a. REPORT SECURITY CLASSIFICATION Unclassified	1b. RESTRICTIVE MARKINGS
2a. SECURITY CLASSIFICATION AUTHORITY	3. DISTRIBUTION/AVAILABILITY OF REPORT Approved for public release; distribution unlimited.
2b. DECLASSIFICATION/DOWNGRADING SCHEDULE	
4. PERFORMING ORGANIZATION REPORT NUMBER(S) TT-71	5. MONITORING ORGANIZATION REPORT NUMBER(S) ESD-TR-88-180
6a. NAME OF PERFORMING ORGANIZATION Lincoln Laboratory, MIT 6b. OFFICE SYMBOL *(If applicable)*	7a. NAME OF MONITORING ORGANIZATION Electronic Systems Division
6c. ADDRESS *(City, State, and Zip Code)* P.O. Box 73 Lexington, MA 02173-0073	7b. ADDRESS *(City, State, and Zip Code)* Hanscom AFB, MA 01731
8a. NAME OF FUNDING/SPONSORING ORGANIZATION Defense Advanced Research Projects Agency 8b. OFFICE SYMBOL *(If applicable)* TTO	9. PROCUREMENT INSTRUMENT IDENTIFICATION NUMBER F19628-85-C-0002
8c. ADDRESS *(City, State, and Zip Code)* 1400 Wilson Boulevard Arlington, VA 22209	10. SOURCE OF FUNDING NUMBERS PROGRAM ELEMENT NO.: 62702E, 62204F PROJECT NO.: 300 TASK NO.: WORK UNIT ACCESSION NO.:

11. TITLE *(Include Security Classification)*
Studies of Target Detection Algorithms That Use Polarimetric Radar Data

12. PERSONAL AUTHOR(S)
L.M. Novak, M.B. Sechtin, M.J. Cardullo

13a. TYPE OF REPORT	13b. TIME COVERED	14. DATE OF REPORT *(Year, Month, Day)*	15. PAGE COUNT
Project Report	FROM _____ TO _____	1988, October 12	64

16. SUPPLEMENTARY NOTATION

17. COSATI CODES		
FIELD	GROUP	SUB-GROUP

18. SUBJECT TERMS *(Continue on reverse if necessary and identify by block number)*
polarimetric radar
target detection
target classification
optimal polarimetric detector
polarimetric matched filter
target models
clutter models

19. ABSTRACT *(Continue on reverse if necessary and identify by block number)*

This report describes algorithms which make use of polarimetric radar information in the detection and discrimination of targets in a ground clutter background. The optimal polarimetric detector (OPD) is derived; this algorithm processes the complete polarization scattering matrix (PSM) and provides the best possible detection performance from polarimetric radar data. Also derived is the best linear polarimetric detector, the polarimetric matched filter (PMF), and the structure of this detector is related to simple polarimetric target types. New polarimetric target and clutter models are described; these models are used to predict the performance of the OPD and the PMF. The performance of these algorithms is compared to that of simpler detectors that use only amplitude information to detect targets. Finally, the ability to discriminate between target types by exploiting differences in polarimetric scattering properties is discussed.

20. DISTRIBUTION/AVAILABILITY OF ABSTRACT	21. ABSTRACT SECURITY CLASSIFICATION	
☐ UNCLASSIFIED/UNLIMITED ☒ SAME AS RPT. ☐ DTIC USERS	Unclassified	
22a. NAME OF RESPONSIBLE INDIVIDUAL Lt. Col. Hugh L. Southall, USAF	22b. TELEPHONE *(Include Area Code)* (617) 981-2330	22c. OFFICE SYMBOL ESD/TML